行政院國家科學委員會專題研究計畫　期中進度報告

有機物、礦物及水在深埋或隱沒沉積物中交互作用之實驗研究(2/3)

計畫類別：個別型計畫
計畫編號：NSC93-2116-M-002-003-
執行期間：93 年 08 月 01 日至 94 年 07 月 31 日
執行單位：國立臺灣大學地質科學系暨研究所

計畫主持人：黃武良

計畫參與人員：賴士禾、張英如、莫慧偵

報告類型：精簡報告
報告附件：出席國際會議研究心得報告及發表論文
處理方式：本計畫可公開查詢

中　華　民　國 94 年 7 月 8 日

行政院國家科學委員會補助專題研究計畫期中報告

※※※※※※※※※※※※※※※※※※※※※※※※※※
※　有機物、礦物及水在深埋或隱沒沉積物中交互作用　※
※　之實驗研究　※
※　※
※※※※※※※※※※※※※※※※※※※※※※※※※※

計畫類別：☑個別型計畫　　□整合型計畫

計畫編號：NSC　93－2116－M－002－003

執行期間：　93 年　8 月　1　日至　94 年　7 月　31 日

計畫主持人：黃武良(wlhuang@ntu.edu.tw)

計畫參與人員：　賴士禾、張英如、莫慧偵

本成果報告包括以下應繳交之附件：

□赴國外出差或研習心得報告一份

□赴大陸地區出差或研習心得報告一份

☑出席國際學術會議心得報告及會議發表講稿一份

□國際合作研究計畫國外研究報告書一份

執行單位：國立台灣大學地質科學系

中　華　民　國　94　年　7　月　8　日

行政院國家科學委員會專題研究計畫期中報告

有機物、礦物及水在深埋或隱沒沉積物中交互作用之實驗研究

計畫編號：NSC 93-2116-M-002-003
執行期限：93 年 8 月 1 日至 94 年 7 月 31 日

主持人：黃武良　國立台灣大學地質科學系
計畫參與人員：賴士禾、張英如、莫慧偵　國立台灣大學地質科學系

The geochemical evolution of carbonaceous matter as a function of temperature, pressure, and other geological factors is essential to our understanding of the fate of organic matter, through a series of geological processes, in burial or subducted sediments. Previous studies focused mostly on the effect of temperatures and pressures on organic reactions with little concern on the influence of other geological factors. This three-year research project covers a series of experimental programs, which will be conducted successively to elucidate several important issues including the effect of mineral-water environments, the effect of type of organic matter, and development of new experimental technique.

Our research in the first year (2003-2004) focuses on the influence of oxidation-reduction condition on the generation of methane and carbon dioxide from organic matter in diagenetic environments. The results have been reported in the 2004 Gordon Research Conference (Organic Geochemistry) and documented in a paper submitted to a SCI journal “Organic geochemistry” (currently in revision; see attachment I).

Our research in the second year (2004-2005) focuses on the visual behavior of organic matter at high temperature and pressures, and the Fourier transform infrared spectroscopy (FTIR) studies of organic matter. The results show that the DAC-pyrolysis technique is useful for identifying the oil vs. gas prone organic matter. The FTIR has been confirmed to be a promising tool for quantifying the extent of organic reactions and determine the change of chemical functionality of the organic matter during transformation, although we are still unable to conduct the *in situ* measurement of IR spectroscopy at high temperature and pressure. These techniques have been applied to a variety of organic matter worldwide, including individual macerals separated from humic coals. The results have been reported in 2004 Annual Meeting of Geological Society of China, and an international conference (ISATT) in July 2005, and have been

documented in a manuscript (see attachment II) to be submitted to a SCI journal "International Journal of Coal Geology". In addition, we have investigated the thermal stability of a carbonaceous matter, fullerene (C_{60}), under geological conditions. The occurrences of nature fullerene have been reported in sediments from K-T and P-T boundary, in black shale and in organic rich rock of greenschist facies. Its stability or kinetics may be used as a potential geothermometer. In this research year, we have conducted preliminary experiments and developed technique to quantify the transformation of C_{60} to amorphous carbon under hydrothermal conditions.

In the third year (2005-2006) of this research project, we shall focus on the kinetics of the transformation of C_{60} to amorphous carbon. In addition, we shall conducted experimental study on the effect of sulfur radical on the kinetics of organic transformation.

Papers derived from researches supported by NSC were published or to be published in SCI journals during the research period (2003-2005) including:

1. Huang, W.L., 2003, The nucleation and growth of polycrystalline quartz: Pressure effect from 0.05 to 3 GPa. European Journal Mineralogy 15, 843-853 (SCI). Impact factor: 1.335.

2. Lin, S.J., Huang, W.L., 2004. Polycrystalline calcite to aragonite transformation kinetics: experiments in synthetic systems. *Contributions to Mineralogy and Petrology* **147**, 604-614. (SCI), impact factor: 2.433

3. Cheng, A.L., W.L., Huang, 2004. Selective adsorption of hydrocarbon gases on clay and organic matter. *Organic Geochemistry* **35**, 413-423. (SCI). impact factor: 1.756.

4. Shen, P.Y., Hwang, S.L., Chu, H.T., Yui, T.F., Pan, C.N., Huang, W.L., 2005. On the transformation pathways of α-PbO2-type TiO2 at the twin boundary of rutile bicrystals and the origin of rutile bicrystals .*European Journal of Mineralogy*. (SCI) (in press).

5. Su, K.W., Huang, W.L., 2005. Generation of hydrocarbon gases and CO_2 from a humic coal: Experimental study on the effect of water, minerals and transition-metals. *Organic Geochemistry*. (in revision)

附件一　Manuscript Submitted to
Organic Geochemistry (in revision)

Generation of hydrocarbon gases and CO_2 from a humic coal: Experimental study on the effect of water, minerals and transition-metals

Kwan-Hwa Su[a] and Wuu-Liang Huang[a]*

[a]*Department of Geosciences, National Taiwan University, Taipei, Taiwan*

Abstract

The yields and composition of hydrocarbon gases and CO_2 generated from a coal were experimentally determined under different litho logical conditions simulated by adding a variety of minerals and transition metals, including hematite, siderite, pyrrhotite, gypsum, Fe, Ni and V in the coal sample using confined hydrous pyrolysis technique. The experiments were conducted at 340 and 360 °C for time durations ranging from 24 to 240 hours. The results reveal that the studied mineral-water environments have a small, but measurable influence on both the yields and composition of the generated gases. The difference in total hydrocarbon gas yields in different mineral environments at the same maturity can be as high as 15 mol. %. The hydrocarbon gas yields, in general, increase slightly with decreasing oxygen activity or increasing hydrogen fugacity of the experiments; this trend becomes more pronounced at higher maturity. Sulfide (pyrrhotite) tends to inhibit slightly the production of hydrocarbon gases while sulfate (gypsum) does not. Carbonate (siderite) or the generated CO_2 exerts an adverse influence on the production of hydrocarbon gases. The effect of mineral environments on the variations of CO_2 yields is more pronounced than that of hydrocarbon gases at the studied conditions. CO_2 production is highest in carbonate and lowest in metallic iron or nickel environments.

*Corresponding author: Tel.: +886-2-33662929; fax: +886-2-83692853
Email address: wlhuang@ntu.edu.tw (W. L. Huang)

1.INTRODUCTION

Accurate characterization of the oil generation potential of source rocks is essential to assess hydrocarbon accumulation in a petroleum system. The amounts and types of organic matter in the source rocks, in addition to temperature and time, determine the yields and composition of the generated hydrocarbons. The roles of these factors have been routinely evaluated in predicting hydrocarbon occurrence in petroleum systems (Tissot et al., 1987; Waples, 1994). However, failure of a prediction, for example the occurrence of hydrocarbon gas in nature at maturity much lower than conventional thought, is not uncommonly encountered, particularly in coal beds (Muscio et al., 1993; Rowe and Muhlenbachs, 1999; Ramaswamy, 2003). Other factors which may play important roles in hydrocarbon generation and its associated organic maturation include the catalytic effects of transition elements, organic-sulfur, minerals or aqueous reactions in the source rocks (Goldstein, 1983; Mango, 1992b; 1997; Helgeson et al. 1993; Lewan 1997; 1998; Seewald 1997; 2001; 2003; Butala et al., 2000; Behar et al. 2003). Mango (1992; 1996) experimentally demonstrated that the generation rate of hydrocarbon gases and their methane contents in the presence of metal-catalysts, are significantly higher than those by conventional pyrolysis technique but close to levels observed in nature. The effect of organic–inorganic interactions, in particular, the availability of hydrogen, on the generation of hydrocarbons in sedimentary basins has been reviewed comprehensively by Seewald (2003).

Among these factors, the role of minerals or aqueous reactions in the source rock in hydrocarbon generation and its associated organic maturation has been increasingly recognized (Helgeson et al. 1993; Lewan 1997; Berndt, et al., 1996; Seewald 1997; 2003; Behar et al. 2003). The high surface area of minerals or clays associated with the organic matter may catalyze the organic maturation (Johns, 1979; 1982); whereas the mineral-water reactions may significantly change the oxygen, sulfur and carbon dioxide activity, and indirectly affect the organic maturation within the sources rocks (Helgeson et al. 1993; Berndt et al., 1996; Seewald, 1997; 2003). Most previous studies on the catalytic experiments were conducted under dry conditions (Brook, 1952; Eisma and Jurg, 1964; Hosfield and Douglas, 1980; Goldstein, 1983; Huizinga et al., 1987; Mango, 1992; 1997), which rarely occurred within natural source rock environments. As the role of water in the generation of petroleum has been increasingly recognized (Hoering, 1984; Siskin and Katritzky, 1991; Lewan, 1997; Seewald 1997), the pyrolysis experiments in the presence of water are believed to more accurately simulate the oil/gas generation and expulsion from source rocks (Barth et al., 1994; Lewan 1997; Behar et al., 1991; 1997; Seewald et al., 1998; Ritter, et al., 1995;

Schimmelmann, et al., 1999). In addition, water is believed to affect the catalytic efficiency; for instance the efficiency of acidic-type catalysts (e.g. clays) can be significantly lowered in the presence of water (Goldstein, 1983; Tannenbaum et al., 1985). The effect is attributed to the difference in reaction mechanism of gas generation: a carbonium-ion mechanism in the absence of water in contrast to a free radical mechanism in the presence of water (Eisma and Jurg, 1969). The extents and mechanism of the catalytic effect of mineral matrices, particularly in the presence of water, however, are still not fully understood.

The present study considers potential natural catalysts which could significantly change the gas generation rate and its composition. We have experimentally measured the yields and composition of gases generated from a humic coal in the presence of water with a variety of minerals or metals, including hematite, siderite, pyrrhotite, gypsum, Fe, Ni and V. Our observations focus on the yields, rates of hydrocarbons and carbon dioxide, the gas compositions, and the isomer distributions.

2. Experimental procedures

2.1 Starting materials

The coal sample was collected by from the coal seam in Shan-Fu-Chi sandstone from the middle Miocene age located at Ming-Ted Dam profile outcropping on the west frank of the Chuhuangkeng anticline in northwestern Taiwan. Petrogtraphic study shows that the coal contains mainly desmocollinite (about 75 %) implying a terrestrial high plant origin. The VR (0.35 %) measured from telecolinite in the sample indicates that it is an immature coal. The geochemical parameters measured using Rock-Eval pyrolysis show that the total organic carbon (TOC), hydrogen index (HI), oxygen index (OI) and *Tmax*, respectively, are 58 %, 273 mg HC/g TOC, 22 mg CO_2/g TOC, and 410 °C. The coal sample was ground in a nitrogen atmosphere to an average size around 40 μm. The powdered samples without special treatments or kerogen isolation, were used throughout the experiments. The minerals and metals (thereafter named as mineral matrices) added to the system including hematite (Fe_2O_3), siderite ($FeCO_3$), pyrrhotite ($Fe_{1-x}S$), gypsum ($CaSO_4.2H_2O$), sylvite (KCl), iorn (Fe), nickel (Ni) and vanadium (V).

2.2 Confined pyrolysis

The experiments were conducted under three confined pyrolysis conditions: confined hydrous, confined non-hydrous and confined dry conditions. Confined pyrolysis was conducted in a closed system using flexure containers, which can be deformed to adjust the sample pressure to equal the externally applied pressure (Monthioux, et al., 1985; Behar, et al., 1991; Landais et al., 1994; Freund et al., 1994). In confined hydrous pyrolysis, water and the solid sample were loaded and sealed within a gold capsule, whereas in confined non-hydrous pyrolysis, no water was added to the sealed capsule (Behar et al., 2003). Although there was no added water in the confined non-hydrous pyrolysis, water may be generated during the early stage of coal pyrolysis in the system (Huang, 1996; Behar et al., 2003). Thus, in confined dry pyrolysis, KCl salt was added along with the coal sample in the gold capsule in order to minimize the activity of water in the system (Newton, 2002) since the salt could dissolve into the water generated during pyrolysis.

All experiments with mineral matrices were conducted under confined hydrous pyrolysis with mass proportion of coal: mineral: water around 3: 1: 1. Powdered coal (about 10 mg) sample with water and mineral matrices water was loaded and electric arc sealed in gold capsules (0.5 mm OD x 15 mm length). For comparison, all coal samples without added mineral matrices were performed in the presence or absence of water. The sample capsules were bound together using platinum wire and loaded into a Parr pressure vessel partially filled with water. The vessel was heated isothermally at 340 and 360 °C for run durations of 24, 72, 240, and 720 hours. In order to prevent the capsules from bursting due to overpressure generated during the gas generation within the capsule, an external argon pressure of 50 bars was applied for runs at 360 °C. The pressure within the gold capsules during the experiments was close to the saturated water vapor pressure for runs at 340 °C and 50 bars above the vapor pressure at 360 °C.

2.3. Analysis of gases and solid pyrolysates

After experiments each cleaned sample capsule was loaded into a glass vial with a gas-tight septum. The free space in the vial was accurately measured with a correction for the volume of solid gold. The capsule was punched with several holes using a stainless needle through the septum in order to release gases into the vial space from the capsule. The analysis was then performed by extracting 0.25 ml of the gas from the vial using a micro-syringe and

injecting it into the inlet of a Gas-chromatograph (GC). The yields of individual gases under different experimental conditions were quantified using a gas chromatograph with FID detector for hydrocarbon gases (HC) and TCD detector for CO_2 in a HP6890 Gas-chromatograph. The capillary column had 0.53 I.D. and 15 m length (HP-Plot Al_2O_3). Chromatographic grade (99.9995%) helium gas was used as carrier gas. The calibration curves for hydrocarbon gas components (C_1 to C_6) were made frequently to quantify the absolute amount of each gas component. The details of analytical procedure were as reported in Cheng and Huang (2004).

The solid pyrolysates were removed from the sample capsule for VR, infrared spectroscopic, x-ray diffraction and scanning microscopic analyses. The VR was measured under an x20 objective lens with oil immersion using a petrographic microscope. The reported reflectance (%Ro) was averaged from about 100 measurements of each sample with very small standard deviation around $\pm$ 0.015. The chemical functionality, particularly aliphatics and aromatics of the solid pyrolysates analyzed using Bomem model DA8.3 Fourier transformed infrared spectroscopy (FTIR). The samples were prepared in KBr pellets containing 0.5% of solid pyrolyzed residues.

3. EXPERIMENTAL RESULTS

3.1. GENERAL REMARKS

Experimental results provide information about the amounts and the composition of hydrocarbon gases (HC gas), and carbon dioxide generated from the coal with different mineral matrices as a function of maturity (Tables 1 to 8). The results show that water activity, the redox conditions and the mineral matrix (sulfide, sulfate and carbonate) have some influence on the gas generation. The absolute and relative yields of individual hydrocarbon gas, methane (C_1), ethane (C_2), propane (C_3), normal butane (n-C_4), iso-butane (i-C_4), pentane (C_5), and hexane (C_6) and CO_2 under different experimental conditions have been quantified and compared. The analysis of liquid hydrocarbons (C_7^+) was not performed due to the insufficient amounts of pyrolyzed residue samples. The thermal maturity of the experimental conditions was determined mainly by the VR measured from the solid residues (Fig 1), which are slightly higher than those calculated from the experimental temperature-time pairs using Easy%Ro (Sweeney and Burnham, 1990).

3.2Hydrocarbon Gas Generation

The experimental results generally show that the cumulative yields of total hydrocarbon gases increase consistently with increasing vitrinite maturity thermally matured at different temperature-time pairs. The generation rate is nearly constant in the early stage but slightly increases at vitrinite maturity above about 1.5 %Ro (Fig. 2). This trend is similar for most studied conditions containing a variety of mineral matrices (Fig. 2). Similarly, methane or each individual wet gas yield increases progressively with increasing maturity and their relative yields are in inverse proportion to their molecular weights (Fig. 3). The proportion of each individual gas varies only slightly in experiments containing the different mineral matrices. The cumulative yields of methane relative to wet gases in terms of $C_1/(C_1+C_2+C_3)$ ratios (Fig. 4) or $C_1/(C_1$ to $C_6)$ percentages (Fig. 5), decrease with increasing maturity up to Ro = 1.42 %, then increase at higher maturity for runs without mineral matrices and with KCl, Fe, and FeS (Fig. 4A). It is noteworthy that the reverse of the trends for experiments containing gypsum, hematite, siderite, nickel and vanadium occurs at vitrinite maturity about 0.1 %Ro higher than other runs (Fig. 4B). In general, a similar trend has also been observed in most runs of this study, although the variation of the ratios is slightly different with different minerals. The $i\text{-}C_4/n\text{-}C_4$ ratios in experiments with coal and water without mineral matrix show a progressive decrease ranging from 1.1 to 0.62 with increasing experimental maturity from 1.15 to 1.9 %Ro (Fig. 6); the change of this ratio appears to be less pronounced at maturity higher than 1.6 %Ro. Similar trends but with wide variation of the ratios have been found in experiments with water and different mineral matrices (Fig. 7).

The effect of water or water activity has been investigated here in three different pyrolysis methods using the coal sample without a mineral matrix. The cumulative yields of total HC gas from the coal at confined dry hydrous condition are only slightly higher than that at confined non-hydrous and confined hydrous conditions (Fig. 8A). It appears that very low water activity in the system tends to slightly enhance the gas generation. The difference in HC gas yields generated from confined hydrous and confined non-hydrous experiments is very small, and may be negligible if experimental uncertainty is considered (Fig. 8A). The cumulative yields of methane relative to wet HC gases as a function of maturity vary only very slightly with water activity. The $i\text{-}C_4/n\text{-}C_4$ ratios in the gas generated in the maturity range of this study, however, are consistently lower in confined non-hydrous experiments than other two methods although the differences are small (Fig. 6).

The experiments show that the variation of hydrocarbon gas yields in the presence of different studied mineral matrix and water, although small, is experimentally significant (Fig.

9). The influence of mineral matrices appears more noticeable at higher maturity; an effect that can be as high as 15 % of total HC gas yield at maturity close to Ro = 1.9 %. The coal sample in experiments with vanadium at 360 °C for 720 hours generated about 15 % more HC gas than in experiments with siderite. The mineral effects on the enhancement of the total HC gas generation increase generally in the order of Fe_2O_3 < FeS < $FeCO_3$ < Ni < added water < $CaSO_4$ < no added water < Fe < dry (KCl) < V (Fig. 9).

The results from two series of experiments containing sulfur show that the one with gypsum yields total HC gas similar to that in pure water but the one with pyrrhotite yields slightly less total HC gas than that with sulfate over the range of maturities studied (Figs. 10A and 10B). The effect of carbonates on gas generation was investigated by a series of experiments with siderite and water. The results when compared with other iron-bearing mineral matrices show that the HC gas yields in the presence of siderite are higher than hematite, but lower than in the presence of iron or magnetite.

3.3. Carbon dioxide generation over a wide range of maturity

The results from runs without minerals show that most CO_2 was generated at maturity lower than Ro = 1.15 %. The cumulative yields increase slightly at the maturity ranging from 1.15 to 1.65 %Ro, then increase at a higher rate at higher maturity (Fig. 11). Similar to the HC gas yields, the difference in CO_2 yields between confined hydrous and non hydrous pyrolysis is negligible whereas the CO_2 yield is slightly lower in confined dry pyrolysis. The addition of minerals, pyrrhotite, sulfate, or hematite in the system shows no significant influence on the CO_2 generation (Fig. 12). In contrast, the CO_2 yield is about 50 % and 30 %, respectively, lower in the presence of iron and nickel and about 10 to 50 % higher in the presence of siderite. The CO_2 yields, in general, increase in order from Fe < Ni < dry (KCl) < V < gypsum < pyrrhotite < no added water < added water< hematite < siderite (Fig 12). This order implies that with a higher oxidation state in the system, there is higher CO_2 yield. Note that the experiments in the presence of siderite produced less CO_2 at low maturity but significantly more CO_2 at high maturity compared to samples in pure water. The CO_2/(CO_2 + HC gas) mol ratio in total gas in confined hydrous pyrolysis decreases progressively with increasing maturity from higher than total HC gas yields at maturity lower than 1.6 %Ro to lower at higher maturity. Similar trends were found for experiments under different conditions (Fig. 13). The CO_2/ (CO_2 + HC gas) mol ratios vary considerably with mineral matrices (Fig. 14).

The effect of mineral matrices on CO_2 generation, in general, is more pronounced than on total HC gas (Fig. 15A and 15B).

3.4. Characterization of solid pyrolysates

The measured reflectances of vitrinite-like materials in the solid pyrolysates in confined hydrous pyrolysis experiments with no added mineral matrix have been used to indicate the maturity of artificial maturation of the studied coal (Fig. 1). The reflectances were compared with those selectively measured in experiments containing gypsum, hematite and vanadium (Fig. 16). The results generally show that the addition of these mineral matirces tends to suppress very slightly, even insignificantly, the vitrinite reflectance (VR) relative to that with water only. At maturity lower than about 1.4%Ro, vanadium suppresses the reflectance most of among these mineral matrices whereas at higher maturity the effects of these mineral matrices vary significantly but with no systematic trend. A dramatic suppression of VR was observed at maturity from 1.9 to 1.72%Ro in experiments with hematite. In addition, a significant suppression of VR in the system containing gypsum has also been observed at high maturity (Fig. 16).

The measured VRs in the solid pyrolysates from confined hydrous pyrolysis and confined non-hydrous pyrolysis experiments with no added mineral matrix were correlated with the results measured by FTIR. The results show that the peak intensity of absorption band ratios of 1500 - 1600 cm^{-1} and 2900 - 3000 cm^{-1}, which approximately represent the relative amount of aromatics to aliphatic functional groups, respectively, increases with increasing maturity (Fig. 17). It appears that the change of the measured functional groups with %Ro is more pronounced in samples with water than those with no water added (Fig. 17). The variation of the absorption band ratio in experiments with different mineral matrices is small except for pyrrhotite and siderite (Fig. 18). It is noteworthy that there is an inverse correlation between the absorption band ratios (aromatics / aliphatics ratio) and the total hydrocarbon yields in the presence of all the mineral matrices except siderite (Fig. 18).

4. Discussion

4.1 Hydrocarbon yields and composition

The yields and composition of laboratory-generated hydrocarbon gas are comparable to those previously reported. Figure 19 compares the methane yield artificially pyrolyzed from a variety of coals as a function of maturity. The methane yield from our studied coal is similar to those derived from Illinois coal # 6 (Vorres, 1990) and Morwell coal (Behar et al., 1995) but slightly lower than that from Mahakam coal (Behar et al., 1995). Calvert lignite generated much lower methane than other coals (Behar et al., 2003). The comparison reveals that the methane yields depend highly on the type and composition of coals.

The effects of mineral matrices revealed in the present study, is small relative to those resulted from the variation of coal types. The relatively small mineral effect on the organic reaction is inconsistent with the results from previously experiments conducted in the dry system (Goldstein, 1983; Mango, 1996). Mango (1996) experimentally demonstrated that the HC gas can be generated at very low thermal stress in the presence of source rocks containing transition metals. Our results, however, suggest that the large catalytic enhancement on the cracking of organic matter containing transition metals (Fe, Ni and V) previously reported has not been observed in our experiments with water during confined pyrolysis. Although the retardation mechanism of water on the catalytic effect is still not clear, these results are consistent with prior studies which predicted that water may significantly reduce the catalytic efficiency of an acid-type mineral surface (Eisma and Jurg, 1969). The loss of efficiency of mineral catalysts in the experiments may also be attributed to the wet ability of the mineral surfaces, which minimizes the contact between organic matter and mineral matrix. The prediction of hydrocarbon gas yields in a petroleum system, therefore, should consider more the coal type than the lithology or mineral matrices associated with the coal.

The mole percentages of methane in the HC gas ranged from 62% to 68% observed in this study, which are consistent with those artificially matured at similar maturities using Mahakam coal in the confined closed system pyrolysis (Michels et al., 2002). These are lower than the methane proportion in HC gas accumulated in natural gas reservoirs (Mango, 1992; 2000; Michels et al., 2002), but higher than those found in source rock cuttings (Snowdon, 2001). The artificial maturation in semi-open system conducted by Michels et al. (2002), however, shows higher proportions of methane (90 to 97%) which are similar to those in reservoir.

The high initial methane proportion and the decrease of the proportion with maturity (Fig. 4) for both the studied coal and the Mahakam coal imply that methane (C_1) is the dominant HC gas generated in the early stage of maturation, while the wet gases formed significantly

only in middle stages. The reverse trend in the late stage, which shows an increase of the methane proportion at higher maturity (>1.42 %Ro), is probably attributed to the secondary cracking of wet gases (C_2 to C_4) or liquid hydrocarbons (C_5+) to form methane, although this does not exclude the likelihood that the reverse of the trend is simply due to the primary cracking of the solid coal. Artificial maturation of Mahakam coal show similar reverse trends at 1.25%Ro and 1.1%Ro, respectively in both closed and semi-open system (Michels et al., 2002). The reverse trends for experiments containing gypsum, hematite, siderite, nickel and vanadium, which occurs at about 1.52 %Ro (Fig. 4B), implies that these minerals or metals may retard the secondary cracking relative to those without mineral matrices or with iron or pyrrhotite. The increase of the C_1/ (C_1 to C_6) ratio and the absolute amount of C_1 at high maturity may be attributed more to the secondary cracking of liquid hydrocarbons (C_5+) or primary cracking of solid residue and less to the wet gases (C_2 to C_4) since the thermal stability of wet gases is higher than the long-chain hydrocarbons or the methyl-bearing aromatics groups in the liquid hydrocarbons (C_5+) (Laidler et al., 1962; McNeil and BeMent, 1996). This interpretation is consistent with the semi-open confined pyrolysis data of Michels et al. (2002) who suggested that the high methane proportion at high maturity may not be attributed to the secondary cracking of wet gases since they were stepwise released out of the system during pyrolysis.

The interpretation of the secondary cracking of liquid hydrocarbons has been supported from data on butane isomers. The initial high i-C_4/n-C_4 ratios (about 1.2) in the HC gas generated at low maturity imply that coal releases i-C_4 at rates faster than n-C_4. The progressive decrease of the ratio from 1.2 to 0.6 as experimental maturity increases to about 1.9 %Ro (Fig. 7) indicates either the decrease of i-C_4 release rate or increase of n-C_4 generation rate with maturity. He'roux et al. (1979) reported that primary cracking of solid organic matter tends to release more iso-butane isomer than normal-butane (with the isomer ratio >0.9) and vice versa (with the ratio < 0.8) during the secondary cracking of oils. The observed decrease of the ratio with maturity in our experiments may partially contribute to the progressive cracking of early formed oil. The decline of the ratio across the boundary (0.8 to 0.9) was observed at maturity around 1.45 %Ro, suggesting significant secondary cracking of liquid hydrocarbons may occur around this maturity. This maturity is consistent with that (1.42%Ro) observed based on the $C_1/(C_1+C_2+C_3)$ ratio (Fig. 4A). This general trend is similar for most conditions in a variety of mineral matrices, although the isomer ratios show significant variation under different conditions.

4.2. Role of water

The HC gas yield in a system with very low water activity (confined dry condition) is about 5 % higher than those in the presence of water (confined non-hydrous and hydrous conditions). This effect, although small, is significant because similar effects were consistently observed in experiments with different maturity. The small retardation by water on the light hydrocarbon generation from coal suggests that most hydrocarbon gases were decomposed from coal molecules rather than secondarily cracked from long-chain hydrocarbons (Lewan, 1997; Seewald, 2003). The water effect, however, is less than that found by Behar et al. (1997; 2003), who showed 13.9 % higher HC gas yield from a lignite in the absence of water (open nonhydrous condition) than in the presence of water (closed nonhydrous condition). Our results, which show no significant difference in gas yields between confined nonhydrous and hydrous conditions are also not consistent with that of Behar et al. (2003), who showed that experiments at closed non-hydrous condition generates more HC gas than at hydrous pyrolysis conditions. This discrepancy may be attributed to different experimental setups. Our confined pyrolysis was performed using flexure containers, which can be deformed to adjust the sample pressure to equal the externally applied pressure whereas Behar et al. (2003) conducted closed pyrolysis in rigid autoclaves. Free water is believed to be present also in the experimental systems under both confined non-hydrous and closed non-hydrous conditions because of the generation of water from organic samples in the early-stage of pyrolysis (Huang, 1996; Behar et al., 2003). The similarity in HC yields generated in our experiments in both confined non-hydrous and hydrous pyrolysis is not unexpected since water pressure is a similar result from the same external pressure. In contrast, the difference in HC gas yields in Behar's experiments was attributed to different water vapor pressures in closed non-hydrous and closed hydrous pyrolysis (Behar et al., 2003). These results imply that water pressure plays a significant role in the HC gas generation (Hill et al., 1994).

The water activity also influences the dryness of the generative gas. The significantly lower proportion of methane in the gas generated at very low water activity than in the presence of water has been observed at maturity lower than 1.6%Ro (Fig. 4A). It appears that water may enhance the release of methyl groups from the coal. However, the effect is reversed at higher maturity, where the secondary cracking of the wet gas prevails, implying

that water may retard the cracking of wet gases to methane. The i-C_4/n-C_4 ratios are consistently higher in runs with excess water, implying that water may enhance preferentially the release of branch alkanes relative to straight chain alkanes from the coal.

4.3. Effect of reduction/oxidation (redox) condition

Our results show that the effect of water on hydrocarbon gas generation is small without added mineral matrices. Water may be involved in the organic reactions if it proceeds hydrolytic disproportional reactions by dissociating into hydrogen and oxygen via mineral-water reactions (Seewald 1997). The present study demonstrates from four series of experiments with different oxygen fugacity in systems where oxygen fugacities in the system which are buffered by minerals at the experimental conditions were calculated (Bethke 1996) or estimated from previously determined values (Ulmer & Barnes 1987). The oxygen fugacity buffered in the system decreases in the order of V-V_2O_3, Fe-Fe_3O_4, Ni-NiO and Fe_3O_4-Fe_2O_3 under the experimental conditions. The results show an increase of total HC gas or methane yields when the oxygen fugacity is decreased or the hydrogen fugacity is increased (Fig. 20A), and the trend is more pronounced at higher maturity (Fig. 20B). The present experiments confirm that the redox conditions indeed influence the gas generation, although the effect is small. The redox potential or hydrogen activity in an aqueous system, therefore, appears to influence HC gas yields in such as a way that excess HC gases may be produced at reducing conditions by reacting excess hydrogen generated from water with organic carbon in the system. However, the present study show that the enhancement of gas yield in the presence of transition metals, Fe, Ni, and V was not as pronounced as previous thought (Mango, 1996; Butala et al., 2000). The discrepancy is probably attributed to the suppression of catalytic effect by water.

4.4 Effect of sulfur

It appears that the presence of sulfur as calcium sulfate in the system has little effect on the HC gas generation (Fig. 10), in contrast to the conventional thought that organic sulfur or sulfur radicals may accelerate organic maturation at lower thermal stress (Baskin and Peters, 1992; Lewan, 1997). These experiments demonstrate that gypsum minerals dehydrate mostly into anhydrite and that there are negligible sulfur products (e.g. H_2S), implying that the

thermal reduction of calcium sulfate by organic matter does not take place in the experiments at high maturity (1.9%Ro) or at high temperature (360 °C). This result contradicts the common observation that the thermochemical sulfate reduction (TSR) can proceed in evaporate-bearing formations at similar or lower maturity. It appears that the high thermal stability and low aqueous solubility of calcium sulfate in the laboratory system generates insufficient amounts of sulfur radicals required for initiation of the catalytic breaking of C-C bonds (Lewan, 1998). The enhancement of TSR reactions in nature, on the other hand, is probably attributed to other catalytic effects, for instance, the high initial H_2S pressure (Machel, 2001). The slight or negligible effects of pyrrhotite on the generation of HC gas yield is surprising because the presence of FeS in the system tends to create conditions more reducing and richer in sulfur radicals. Both of these two conditions should favor HC formation.

4.5. CO_2 generation

That the CO_2/CH_4 ratio decreases progressively with increasing maturity is mainly attributed to the continuous generation of hydrocarbon gases as the rate of CO_2 generation tends to decline. This observation is consistent with the previous thought that the generation of CO_2 from type III organic sources takes place at an earlier stage of organic maturation than methane during laboratory pyrolysis and natural catagenesis (Hunt, 1996). The CO_2 yields from runs (with KCl) at very low water activity are slightly lower than that in the presence of water, suggesting that water contributes oxygen to the formation of carbon dioxide.

These results suggest that the mineral-water reactions have been involved in CO_2 generation in these experiments, either by releasing the CO_2 from siderite or by consuming oxygen within organic matter. The later process may compete with the formation of oxides from Fe or Ni. The results show that significant decomposition of siderite into CO_2 and iron oxides (magnetite and hematite) has taken place under the experimental conditions. The decomposition of siderite in the experiments was confirmed by the high CO_2 yield in a high maturity experiment (%Ro = 1.90) containing about double amounts of siderite. By contrast, the presence of reducing agents such as Fe, V and pyrrhotite seems to retard the formation of CO_2. These results suggest that the mineral-water reactions have been involved in CO_2 generation in these experiments.

4.6. Vitrinite reflectance and infrared absorption of solid pyrolysates

Thermal maturity for each set of experimental conditions was approximately represented by the reflectance (%Ro) measured from the vitrinite-like materials in solid run products conducted under confined hydrous pyrolysis. The measured VRs are slightly higher than those calculated from the corresponding temperature and time of experiments using the Easy%Ro program (Sweeney and Burnham (1990) (Fig. 1). This difference is not unexpected since the calculated VR was calibrated against natural samples at temperatures much lower than laboratory temperatures. For application of the experimental data to the prediction of the gas yields and composition in nature, we recommend using the calculated VR because the measured vitrinite was matured at high temperature. The kinetic extrapolation to natural conditions can not be done due to the lack of sufficient data in the study.

Based on limited types of the studied mineral matrices, the very slight suppression of VR in the run products in experiments containing gypsum, hematite and vanadium suggests that the inorganic environments in shales relative to coals may not be an important factor affecting the vitrinite maturation. However, the observed suppression of VR in the presence of gypsum and hematite at high maturity may imply that a high oxic environment tends to suppress the maturation of vitrinite. If this is the case, the slight suppression of VR in the presence of reducing environment, vanadium, at maturity below 1.43%Ro is hard to explain. Further studies are required to determine the effects of mineral matrices on the variation of vitrinite reflectance under similar thermal stress.

The correlation of the measured VR with the aromatics/aliphatics ratio measured by FTIR is not unexpected since the increase of VR is attributed to the aromatization of the organic matter (Rouxhet et al., 1978). Similar observations have been previously reported (Rouxhet et al., 1978; Landais, 1995 Riesser et al., 1984). Landais (1995) found a nice correlation for coals. The good correlation is consistent with most previous studies on the aromatization of organic matter during maturation (Riesser et al., 1984; Benkhedda et al., 1992; Machnikowska et al., 2001). However, micro-FTIR data on vitrinite maceral show significant scattering from the trend (Lin and Ritz, 1993). The poor correlation has also been observed in type-III organic matter (Ganz and Kalkreuth, 1987). The results from our experiments demonstrates that the maturation of a single source of starting vitrinite may generate a more consistent trend. The observed scattering of the data from the trend or the

poor correlation of the trend is probably attributed to the composition variation of starting vitrinite particles in the sample.

The inverse correlation between the amount of HC gas generated and the aromatics/aliphatics group ratio (Fig. 18) may be coincidental but that dose not exclude a possible unknown mechanism which relates to the catalysis of minerals. It appears that the generation of HC gases may retard the aromatization of organic matter. Since more total hydrocarbon gas yields were found in reducing environments, the retardation of aromatization may be due to the higher reducing environment.

5. Conclusions

This study experimentally demonstrated that the mineral-water reactions can influence the yields and composition of hydrocarbon gases and CO_2 generated from a humic coal. The proposed mineral-water reactions which may influence the gas generation include the oxidation-reduction between metal and oxide, sulfate-sulfide conversion, and carbonate decomposition. The extent of influence, although small, depends on the mineral type or mineral-water reactions. The decrease of water or oxygen activity tends to enhance slightly the total hydrocarbon gas yield while the presence of carbonate (siderite), carbon dioxide, and sulfide (pyrrhotite) tends to inhibit slightly the production of hydrocarbon gases. To date, the results based on limited data from some representative minerals and transition metals show a maximum variation of about 15 % for hydrocarbon gas yields during aqueous reactions at maturity equivalent to vitrinite reflectance of about 1.95%. The effect of transition metals is not as pronounced as previously reported at dry condition. The effect of mineral environments on the variations of CO_2 yields is more pronounced than that of hydrocarbon gases at the studied conditions. CO_2 production is highest in carbonate and lowest in metallic iron or nickel environments. This study confirms the previous thought that mineral-water reactions may play a role in natural gas generation in a petroleum system but this study shows that the influence of mineral matrices is small relative to that imposed by the compositional variation of organic matter.

Acknowledgements

This research was supported by the Earth Sciences Sections, National Sciences Council of ROC, NSC Grant 92-2116-M002-018 to W. L. Huang. The authors would like to

acknowledge Mr. Jun-Chin Shen of EDRI, Chinese Petroleum Corporation for supplying the starting coal samples and performing the Rock-Eval pyrolysis and vitirinite reflectance measurement. Thanks are extended to Drs. C. L. Kuo J. N. Weng and T. Y. Yang for reviewing on early version of the manuscript.

References

Aranovich, L.Ya. Newton, R.C., 1996. H_2O activity in concentrated NaCl solutions at high pressures and temperatures measured by the brucite-periclase equilibrium. Contributions to Mineralogy and Petrology 125, 200-212.

Barth, T., Schmidt, B.J., Nielsen, S.B., 1996. Do kinetic parameters from open pyrolysis describe petroleum generation by simulated maturation? Bulletin of Canadian Petroleum Geology 44, 446-457.

Baskin, D.K., Peters, K.E., 1992. Early generation characteristics of a sulfur-rich Monterey kerogen. Amer. Assoc. Petrol. Geol. Bull. 76, 1-13.

Behar, F., Kressmann, S., Rudkiewicz, J.L., 1991. Experimental simulation in a confined system and kinetic modeling of kerogen and oil cracking. Organic Geochemistry 19, 173-189.

Behar, F., Lewan, M.D., Lorant, F., Vandenbroucke, M., 2003. Comparison of artificial maturation of lignite in hydrous and nonhydrous conditions. Organic Geochemistry 34, 575-600.

Behar, F., Vandenbroucke, M., Teermann, S.C., Hatcher, P.G., Leblond, C., Lerat, O., 1995. Experimental simulation of gas generation from coals and marine kerogen. Chemical Geology 126, 247-260.

Behar, F., Vandenbroucke, M., Tang, Y., Marquis, F., 1997. Thermal cracking of kerogen in open and closed systems: determination of kinetic parameters and stoichiometric coefficients for oil and gas generation. Organic Geochemistry 26, 321-339.

Benkledda, Z., Landais, P., Kister, J., Dereppe, J.M., Monthioux, M., 1992. Spectroscopic analysis of aromatic hydrocarbons extracted from naturally and artificially matured coals. Energy & Fuels 6, 166-172.

Berndt, M.E., Allen, D.E., Seyfried, W.E., Jr., 1996. Reduction of CO_2 during serpentinization of olivine at 300 degrees C and 500 bar. Geology 24, 351-354.

Bethke, C.M., 1996. Geochemical Reaction Modeling, Concepts and Application. Oxford University Press, New York.

Brooks, B.T., 1952. Evidence of catalytic action in petroleum formation. Indust. Eng. Chem. 44, 2570-2577.

Butala, S.J., Medina, J.C., Taylor, T.Q., Andrus, D.B. Bartholomew, C.H.,Lee,M. L., 2000. Mechanism and kinetics of reactions leading to natural gas formation during coal maturation. Energy Fuels 14, 235-259.

Cheng, A.L., Huang, W.L., 2004. Selective adsorption of hydrocarbon gases on clays and organic matter. Organic Geochemistry 35, 413-423.

Eisma, E., Jurg, J.W., 1969. Fundamental aspects of the generation petroleum. In: Eglinton, G., Murphy, M.T.J.(eds.), Organic geochemistry; methods and results. Springer-Verlag, New York, pp. 676-698.

Ganz, H., Kalkreuth, W., 1987. Application of infrared spectroscopy to the classification of kerogen-types and the evaluation of source rock and oil shale potentials. Fuel 66, 708-711.

Goldstein, T.P., 1983. Geocatalytic reactions in formation and maturation of petroleum. Amer. Assoc. Petrol. Geol. Bull. 67, 152-159.

Helgeson, H.C., Knox, A.M., Owens, C.E., Shock, E.L., 1993. Petroleum, oil field waters, and authigenic mineral assemblages: Are they in metastable equilibrium in hydrocarbon reservoirs? Geochimica et Cosmochimica Acta 57, 3295-3339.

Heroux, Y., Chagnon, A., Bertrand, R., 1979. Compilation and correlation of major thermal maturation indicators. AAPG Bulletin 63, 2128-2144.

Hill, R.J., Jenden, P.D., Tang, Y.C., Teerman, S.C., Kaplan, I.R., 1994. Vitrinite Reflectance as a Maturity Parameter: Applications and Limitations. In: Mukhopadhyay, P.K., Dow, W.G. (Eds.), American Chemical Society Symp. Ser. 570, pp. 161-193.

Hoering, T.C., 1984. Thermal reactions of kerogen with water, heavy water and pure organic substances. Organic Geochemistry 5, 267-278.
Horsfield, B., Douglas, A.G., 1980. The influence of minerals on the pyrolysis of kerogens. Geochimica et Cosmochimica Acta 44, 1119-1132.
Huang, W.L., 1996. Experimental study of vitrinite maturation: effects of temperature, pressure, time, water and hydrogen index. Organic Geochemistry 24, 233-241.
Huizinga, B.J., Tannenbaum, E., Kaplan, I.R., 1987. The role of minerals in the thermal alteration of organic matter — III. Generation of bitumen in laboratory experiments. Organic Geochemistry 11, 591-604.
Hunt, J.M., 1996. Petroleum Geochemistry and Geology, 2nd Edtion. Freeman, New York..
Johns, W.D., 1979. Clay mineral catalysis and petroleum generation. Ann. Rev. Earth Planet. Sci. 7, 183-198.
Johns, W.D., 1982. Clay mineral catalysis and petroleum generation . AAPG bulletin 66, 1445.
Jurg, J.W., Eisma, E., 1964. Petroleum hydrocarbons; generation from fatty acid. Science 144, 1451.
Laidler, K.J., Sagert, N.H., Wojciechowske, B.W., 1962. Kinetics and mechanisms of the thermal decomposition of propane. Proc. R. Soc. Lond. 270, 242-253.
Landais, P., 1995. Statistical determination of geochemical parameters of coal and kerogen macerals from transmission micro-infrared spectroscopy data. Organic Geochemistry 23, 711-720.
Landais, P.L., Michels, R., Elie, M., 1994. Are time and temperature the only constraints to the simulation of organic matter maturation? Organic Geochemistry 22, 617-630.
Lewan, M.D., 1997. Experiments on the role of water in petroleum formation. Geochimica et Cosmochimica Acta 61, 3691-3723.
Lewan, M.D., 1998. Sulphur-radical control on petroleum formation rates. Nature 391, 164-166.
Lin, R., Ritz, G.P., 1993. Studying individual macerals using i.r. microspectroscopy, and implications on oil versus gas/condensate proneness and "low-rank" generation. Organic Geochemistry 20, 695-706.
Machel, H.G., 2001. Perspectives on investigations of diagenesis for hydrocarbon exploration and exploitation in deep basins. Schriftenreihe der Deutschen Geologischen Gesellschaft 13, 4-7.
Machnikowska, H., Krzton, A., Machnikoski, J., 2002. The characterization of coal macerals by diffuse reflectance infrared spectroscopy. Fuel 81, 245-252.
Mango, F.D., 1992. Methane concentrations in natural gas; the genetic implications. Organic Geochemistry 32, 1283-1287.
Mango, F.D., 1992. Transition metal catalysis in the generation of petroleum and natural gas. Geochimica et Cosmochimica Acta 56, 553-555.
Mango, F.D., 1996. Transition metal catalysis in the generation of natural gas. Organic Geochemistry 24, 977-984.
Mango, F.D., 1997. The catalytic decomposition of petroleum into natural gas. Geochimica et Cosmochimica Acta 61, 5347-5350.
Mango, F.D., 1997. The light hydrocarbons in petroleum; a critical review. Organic Geochemistry 26, 417-440.
Mango, F.D., 2000. The origin of light hydrocarbons. Geochimica et Cosmochimica Acta 64, 1265-1277.
McNeil, R.I., BeMent, W.O., 1996. Thermal stabilities of hydrocarbons: laboratory criteria and field examples. Energy Fuels 10, 60-67.
Monthioux, M., Landais, P., Monin, J-C, 1985. Comparison between natural and artificial maturation series of humic coals from the Mahakam delta, Indonesia. Organic Geochem. 8, 275-292.

Muscio, G.P.A. Horfield, Welte, D.H., 1994. Occurrence of thermogenic gas in the immature zone – implications from the Bakken in-source reservoir system. Organic Geochemistry 22, 461-476.

Price, L.C., Schoell, M., 1995. Constraints on the origins of hydrocarbon gas from compositions of gases at their site of origin. Nature 378, 368-371.

Ramaswamy, G., 2003. A field evidence for mineral-catalyzed formation of gas during coal maturation. Oil and Gas Journal 100-38, 32-36.

Raymond, M., et al., 2002. Understanding of reservoir gas compositions in a natural case using stepwise semi-open artificial maturation. Marine and Petroleum Geology 19, 589-599.

Riesser, B., Starsinic, M., Squires, E., Davis, A., Painter, P.C., 1984. Determination of aromatic and aliphatic CH group in coal by FTIR. II. Studies of coals and vitrinite concentrates. Fuel 63, 1253-1261.

Ritter, U., Myhr, M.B., Vinge, T., Aareskjold, K., 1995. Experimental heating and kinetic models of source rocks: Comparison of different methods. Organic Geochemistry 23, 1-9.

Rouxhet, P.G., Robin, P.L., 1978. Infrared study of the evolution of kerogens of different origins during catagenesis and pyrolysis. Fuel 57, 533-540.

Rowe, D., Muhlenbachs, A., 1999. Low temperature thermal generation of hydrocarbon gases in shallow shales. Nature 398, 61-63.

Schimmelmann, A., Lewan, M.D., Wintsch, R.P., 1999. D/H isotope ratios of kerogen bitumen, oil, and water in hydrous pyrolysis of source rocks containing kerogen types I, II, IIS, and III. Geochimica et Cosmochimica Acta 63, 3751-3766.

Seewald, J.S., 1997. Mineral redox buffers and the stability of organic compounds under hydrothermal conditions. Mat. Res. Soc. Symp. Proc. 432, 317-331.

Seewald, J.S., 2001. Aqueous geochemistry of low molecular weight hydrocarbons at elevated temperatures and pressures: constraints from mineral buffered laboratory experiments. Geochimica et Cosmochimica Acta 65, 1641-1644.

Seewald, J.S., 2003. Organic-inorganic interactions in petroleum-producing sedimentary basins. Nature 426, 327-333.

Seewald, J.S., Benitez-Nelson, B.C., Whelan, J.K., 1998. Laboratory and theoretical constraints on the generation and composition of natural gas. Geochimica et Cosmochimica Acta 62, 1599-1617.

Siskin, M., Katritzky, A.R., 1991. Reactivity of organic compounds in hot water: Geochemical and technological implications. Science 254, 231-237.

Snowdon, L.R., 2001. Natural gas composition in a geological environment and the implications for the processes of generation and preservation. Organic Geochemistry 32, 913-931.

Sweeney, J.J., Burnham, A.K., 1990. Evaluation of a simple model of vitrinite reflectance based on chemical kinetics. Am. Assoc. Petroleum Geol. Bull. 74, 1559-1570.

Tannenbaum, E., Kaplan, I.R., 1985. Low-M hydrocarbons generated during hydrous and dry pyrolysis of kerogen. Nature 317, 708-709.

Tissot, B., Durand, B., Epitalie, J., Combaz, A., 1987. Thermal history of sedimentary basins, maturation indices, and kinetics of oil and gas generation. Am. Assoc. Petroleum Geologists Bulletin 58, 499-506.

Ulmer, G.C., Barnes, H.L., 1987. Hydrothermal Experimental Techniques. John Wiley & Sons, New York.

Vorres, K.S., 1990. The eight coals in the Argonne Premium coal sample program. Energy & Fuels 4, 420-426.

Waples, D. W., 1994. Modeling of the petroleum system-from source to trap. In: Magoon, L.B., et al. (Eds.), The petroleum system; from source to trap. American Association of Petroleum Geologists, Tulsa, pp. 307-322.

Figure Captions

Figure 1. The measured vitrinite reflectance (VR) correlated with those calculated using Easy%Ro (Sweeney and Burnham, 1990). The corresponding temperature- time pair of experiments for each measured VR is: 1.13% (340^{o}C-24hr), 1.26 % (340 ^{o}C-72 hr), 1.34% (360 ^{o}C-24 hr), 1.43% (340 ^{o}C-240 hr), 1.52% (360^{o} C-72 hr), 1.62% (360 ^{o}C-240 hr), 1.90% (360 ^{o}C-720 hr), where hr = hours. The measured VRs were derived from experiments with water but no mineral matrix.

Figure 2. Experimental data showing the cumulative yields of total hydrocarbon gas generated from the studied coal as a function of measured VR. Experiments were carried out at 340 ^{o}C (solid triangles) and 360 ^{o}C (solid circles) and with water and a variety of mineral matrices: A) KCl salt, B) coal only without added water and mineral matrix, C) added water but no mineral matrix, D) gypsum, E) pyrrhotite, F) vanadium, G) iron, H) nickel, I) hematite, J) siderite.

Figure 3. Methane or individual wet hydrocarbon gas yield increases progressively with increasing maturity. Their relative yields are in inverse proportion to their molecular weights.

Figure 4. Experimental data showing the methane/(methane + ethane + propane) ratio i.e. $C_1/(C_1+C_2+C_3)$ ratio, as a function of maturity, in terms of measured VR (%Ro): (A) runs without mineral matrices and runs with FeS and Fe, (B) runs with $CaSO_4$, Ni, Fe_2O_3, $FeCO_3$, and V.

Figure 5. Experimental data showing the percentage of individual gas in total HC gases (C_1-C_6) as a function of maturity (measured VR).

Figure 6. Experimental data showing the ratio of n-butane/ (i-butane + n-butane), i.e. $nC_4/(iC_4 + nC_4)$, as a function of maturity (measured VR). Symbols: Triangles = coal + added water; squares = coal with no water added; diamonds = coal + KCl (very low water activity).

Figure 7. i-butane/n-butane ratios in experiments with water and different mineral matrices.

Figure 8. Experimental data showing the effects of water and maturity on (A) the HC gas yield, and (B) carbon dioxide yields. Symbols for maturity (measured %Ro) : solid rhombs

=1.13%; solid triangles = 1.26 % ; solid circles = 1.34% ; open triangles = 1.42%; open squares = 1.52% ; open circles = 1.62%; solid squares = 1.90%. The corresponding temperature and time pair of experiments for each VR see the legend of Fig. 1.

Figure 9. Experimental data compared among the total hydrocarbon gas yields pyrolyzed under a variety of conditions arranged in the order of increasing hydrocarbon yields. Maturity symbols see Fig. 8.

Figure 10. Experimental data showing the effect of sulfide, sulfates, carbonates on (A) the total hydrocarbon yields. Maturity symbols see Fig. 8, and (B) methane yields as a function of maturity.

Figure 11. Cumulative carbon dioxide yield as a function of measured VR under different conditions.

Figure 12. Cumulative carbon dioxide yield under different conditions at different maturity. Maturity symbols see Fig. 8.

Figure 13. Percentages of CO_2 in the total gas generated from the coal as a function of measured VR.

Figure 14. Experimental data showing the $CO_2/(CO_2 +$ total HC gas) mol ratio under a variety of conditions arranged in the order of increasing hydrocarbon yields. Maturity symbols see Fig. 8.

Figure 15. Experimental data showing the effect of siderite, sulfate or iron or magnetite on (A) the CO_2 yields. Maturity symbols see Fig. 8, and (B) $CO_2/(CH_4)$ ratio of the coal as a function of maturity.

Figure 16 . Experimental data showing the effect of oxidation/reduction potential (hematite vs. vanadium) and sulfates (gypsum) on the VR measured for the solid products. Maturity symbols see Fig. 8

Figure 17. Experimental data showing the change of functionality (aromatic/alkane) ratio as a function of maturity. The intensity ratio of adsorption bands, 1500-1600 cm-1 and 2900-3000 cm-1 measured by FTIR. The ratio represents approximately the ratio of amounts of aromatic to saturates, respectively, in the solid residues. Symbols: triangle = with water; rhomb = no added water.

Figure 18. Experimental data showing the effect of mineral matrices on the aromatics/saturates ratio in solid residue at 360 ^{o}C and 240 hours (measured %Ro = 1.62). The total hydrocarbon yields (triangles) at same conditions were presented for comparison.

Figure 19. Comparison of methane yields artificially generated from a variety of coals. Symbols: open circles = Illinois coal # 6 (Vorres, 1990); solid rhombs = Morwell coal (Behar et al., 1995); open squares = Mahakam coal (Behar et al., 1995); open triangles = Calvert lignite (Behar et al., 2003); solid triangles = Sahnfuchi coal (this study).

Figure 20. Experimental data showing the effect of oxidation/reduction potential under pyrolysis on the total hydrocarbon yields. Maturity symbols see Fig. 8.

附件二　Manuscript to be submitted to

International Journal of Coal Geology

Generation and expulsion of petroleum from coal macerals visualized *in-situ* during semi-open and closed system pyrolysis

F. J. Mo[a], Wuu-Liang Huang[a,*], Jack Machnikowski[b]

[a]*Department of Geosciences, National Taiwan University, Taipei, Taiwan, ROC*

[b]*Institute of Chemistry and Technology of Petroleum and Coal, Wroclaw University of Technology, Gdanska 7/9, 50-344 Wroclaw, Poland*

Abstract:

The oil and gas generative potential of lipinites, vitrinites and fusinites separated from coals of different maturity have been characterized using the diamond anvil cell pyrolysis technique in semi-open and closed systems. The visualization of samples *in-situ* during pyrolysis shows that lipinite generated large amounts of visible oil-like liquid along with some gas while fusinites generated no visible liquid and gas. The liquid (oil) from lipinite appears light in color and less viscous. In contrast, some non-perhydrous vitrinite unexpectedly generated large amounts of visible liquid although the liquid is darker and thicker than that from lipinite, indicating that the oil potential of vitrinites is not limited to its perhydrous nature. The peak temperatures (T_{peak}) of maximum rate of liquid generation for vitrinite (465 to 540 °C) are generally higher than those for lipinites (453 to 475 °C); both of which are within the range of Rock-Eval T_{max} for most organic matter. The visual phenomena and T_{peak} of liquid generation in the closed system are essentially similar to those in a semi-open system, whereas the gas generation appears more noticeable in a closed system. Since semi-open experiments are much easier to perform, the DAC pyrolysis may be routinely conducted in semi-open system if only oil generation is considered.

1. Introduction

Evaluation of oil generation potential of source rocks in a petroleum system is essential to the success of exploration. There are increasing evidences showing that some terrestrial coals, in addition to lacustrine and marine source rocks, may be an important source for oil (e.g. Durand and Paratte, 1983; Hunt, 1991; Law and Rice, 1993; Scott and Fleet, 1994; Wilkins and George, 2002). The oil potential of a coal depends mainly on its maceral constituents (Hunt, 1996). Lipinite (exinite) is the major component that contributes oil for many oil-prone coals (e.g. Indonesia and Malaysia coals, Land and Jones, 1987; Stankiewicz et al., 1996) whereas the perhydrous vitrinite contributes oil for vitrinite –rich but lipinite-poor coals (e.g. New Zealand, Newman et al., 1997; San Juan Basin, New Mexico, Clayton et al., 1991; Gipsland coals, Smith and Cook, 1984; Moore et al., 1992). However, it is still uncertain whether the perhydrous nature of vitrinite is the only source to account for the oil potential of vitrinite-rich coals. Other submaceral components of vitrinite may contribute the oil generation potential.

While the distinction between oil-prone and gas-prone coals become a common practice in the source rock evaluation (Wilkins and George, 2002), the uncertainty about the expulsion or primary migration of oil from coals has caused an additional problem that hinders the accurate evaluation of petroleum potential. Most of techniques including pyrolysis-Gas chromatography (PY-GC; Bertrand, 1989; Powell et al., 1991), elemental analysis (Peper and Corvi, 1995), Rock-Eval pyrolysis (Baskin, 1997), maceral discrimination (Huang et al., 1997) , and spectroscopy (Miknis et al., 1981; 1996; Qin et al., 1991; Machnikowska et al., 2002), which used routinely in the measurements of the oil generation potential of source rocks or coals, are incapable of investigating the expulsion efficiency of oil from coals. The diamond anvil cell (DAC) pyrolysis (Huang, 1996; Weng et al., 2003) and hydrous pyrolysis technique (Lewan, 1997) among a few methods enable to study concurrently both the generation and expulsion of oil from sources rocks. The visual capability of the DAC technique provides the direct observations which enables to show how oil and gas generated and expulsed from a source rocks sample during pyrolysis. In this paper, we present the visual characteristics during pyrolysis of three major types of maceral using separated concentrates from 8 Polish coals. The use of high purity maceral concentrates permits the comparison of the oil and gas generation and expulsion of the individual macerals while minimizing the interference by the presence of other macerals.

2. Experimental methods

2.1 Starting materials

The macerals samples used are the same as in Machnikowska et al. (2002) and were

isolated from 8 coals of different ranks, from subbituminous to anthracite, containing 77.0 to 92.5% °C. The anthracite (sample C41) comes from Lower Silesian Basin, whereas the others come from Upper Silesian Basin. According to Polish classification, the coals represent the types with increasing rank in the order of flame coal (C31.2), gas coal (C33), gas-coking (C34), orthocoking (C35.2), semicoking (C37.1 and C37.2), semianthracite (C41), and anthracite (C42). The coals were separated into three major fractions namely vitrinite, lipinite and fusinite. Maceral separation was performed first by isolation of lithotypes by handpicking, and enriched by float-sink method. Lithotypes was then separated in centrifuge and examined by microscopic analysis for separation efficiency. The final separation products were dried in a vacuum oven at 60 °C. The detailed maceral separation and characteristics of the studied samples including proximate, ultimate analyses of coals and maceral structure revealed by diffuse reflectance infrared spectroscopy are reported in Machnikowska et al. (2002). The proximate, ultimate and petrographic, analyses of the studied macerals conducted by Machnikowska et al. (2002) were presented in Tables 1 and 2. The atomic ratios for hydrogen carbon and oxygen were plotted on a van Krevan diagram (Fig. 1).

2.2 Diamond anvil cell pyrolysis technique

The diamond anvil cell (DAC) pyrolysis techniques (Huang, 1996; Huang and Otten, 1998; Weng et al., 2003) (Fig. 2) was used to simulate maturation of a variety of coal macerals and record the whole reaction process *in-situ*. The whole process of oil and gas generation and expulsion from macerlas can be visually observed. The qualitative and semi-quantitative information has been obtained from the dynamic images. The variation and the yields of oil and gas can be quantified by measuring the volume in terms of the spreading area of the generated liquid phase during the pyrolysis (Weng et al., 2003).

The diamond anvil cell pyrolysis technique and sample configurations are similar to that described in Huang (1996) and Weng et al. (2003). A more detailed sketch of the cell configuration was presented in Bassett et al. (1993) and Huang et al. (1994). A standard petrographic microscope with some modifications has been used for real time visualizing the sample. Real time video recording of experiments is accomplished with a high-resolution CCD (charge coupled device) color video camera and time lapse VCR (Fig 2).

Temperatures were measured using chromel-alumel thermocouples with their junctions closely contacting the pavilion faces of the diamond anvils; they are considered to be accurate to ± 3°C. To prevent oxidation of the heating wires and diamonds at high temperatures, argon gas with 1 % hydrogen was circulated around the heating elements. The heating rates (10 °C/min. up to 300°C, held for 5 min., then at 25 °C/min up to 550 °C), unless specified, are similar to the standard Rock-Eval pyrolysis (set at 300 °C for 5 min., then at 25 °C/min.).

The experiments were conducted under semi-open and closed system conditions. For the semi-open system, the sample with a size about 0.5 mm in diameter was loaded between diamond faces and pressed by the weight of upper diamond set. The anvil pressure ranges from ambient pressure at the sample margin to about 200 MPa at the center (Weng et al., 2003). The sample pressure may slightly increase with increasing the pyrolysis temperature due to the generation of liquid and gases; the pyrolysis experiment can be considered as semi-open system pyrolysis. It is likely that the newly generated volatile liquid or gas may escape from the system while the non-volatile liquid retains, and cracks to gas at higher temperatures, in the system during the pyrolysis. For closed-system experiments, the sample chamber of the DAC consists of a 500 μm diameter hole in a disk-shaped rhenium gasket (125 μm thick and 3 mm OD) sandwiched between two diamond anvils (Fig. 3). Three to four batches of each sample was loaded within the gasket chamber. The sample pressure may slightly increase with increasing the pyrolysis temperature due to the generation of liquid and gases.

2.3 Criteria for Interpretation of visual characters

The observations and characterization of organic samples during DAC pyrolysis focused on the followings:

(1) *The presence or absence of oil and/or gas*. Oil was considered to be present if the sample show softening, corner rounding and spreading of liquid lobes during pyrolysis. The presence of gas was recognized mostly as bubbles within the liquid phase or if the solid sample disintegrated or shrunk during the pyrolysis. However, we used "invisible" instead of absence if none of the above criteria was observed because its absence can not be certain.

(2) Oil yield in semi-open system during pyrolysis was estimated by the ratio of the maximum sample area (A) to the initial sample area (A_o); the initial sample area was measured at 300 °C. We assigned four yield ranks from 1 to 4 corresponding to the ratios of A/A_o of less than 2, between 2 and 3, between 3 and 4, and larger than 4, respectively. For the closed system, the estimation of yield is somewhat difficult. The oil yield was assigned as rank 1 if sample shows only corner rounding without spreading of liquid; it is assigned as rank 2 if liquid spreads around the sample but does not reach the chamber boundary, and as

rank 3 if the spread liquid just touched the chamber boundary. Further spreading of the liquid was designed as rank 4.

(3) Stickiness or fluidity of oil: Stickiness was designed as “light” when oil appears clear or translucent and spreads fluently like water or light crude oil whereas it was designed as “thick” when oil show viscous and move slowly like heavy crude oil. Medium represents that between light and thick.

(4) Reaction rate is estimated based on the time or temperature interval from the beginning to the end of the liquid generation. In semi-open system, it ranks as “fast” if the generation interval is less than 2.5 minutes (or 60 °C interval) and as “slow” if lager than 6 minutes (or 150 °C). “Medium” was assigned for the time intervals between “fast” and “slow”. The reaction interval in the closed system is generally lower than that in the semi-open system. The generation of oil in the closed system is “fast” if it completed within 30 °C interval and “slow” if last longer than 70 °C interval.

(5) Peak temperature of oil generation rate (T_{peak}) is the temperature at which the rate of oil generation is maximum. This temperature was determined by the cumulative oil yield which was in turn estimated by the area of oil spread on the diamond anvil face similar to the method reported by Weng et al. (2003). Figure 4 is an example using lipinite sample E34.

3. Experimental Results

3.1 Semi-open system pyrolysis

While the video show is the best way to observe and interpret the evolution of visual character of the samples in response to pyrolysis temperatures, this paper presents only a sequence of images from the selected samples to show the major features useful for readers to understand and interpret. Figure 5 shows four representatives for lipinite (E34), vitrinite (V33 and V35.1) and fusinite (F34) samples. Two vitrinite samples were presented in order to show two major contrasts in visual change of vitrinite. Three successive images from each sample represent three stages of pyrolysis. The first image indicated by “Initial” was taken at 300 °C to represent the visual appearance before the generation of oil. The second image indicated by “Maximum” shows the feature when the maximum yield of oil has been generated. The third image indicated by “End” was taken at 550 °C to show the appearance of sample near the end of the experiment. The interpretation of the dynamic images were summarized in Tables 3 to 5, and described briefly below.

The initial lipinite samples (E31.1, E31.2, E33 and E34) within the cell under microscope appear as fine-grained aggregates with dark, translucent brown color. The transmission of

light through the sample was enhanced because the sample is thin and less pores due to the press of sample between two diamond anvil faces in semi-open system. Their visual appearance evolved continuously from about 330 °C to 510 °C during pyrolysis. The generative oils are clear and light brownish and its stickiness ranges from “light” to “medium”; the yields of oil are fertile and rank as 3 and 4. Gas generation from all lipinite samples has been recognized by the presence of small bubbles, which continuously evolve through liquid phase and escape out of sample cell concurrently during liquid formation. The reaction rates of oil and gas generation rank as “fast”. The peak temperatures (T_{peak}) located within the range from 450 to 475 °C. Among the lipinite macerals, sample E34 yielded most oil while the E31.2 yielded least oil. At the end of each experiment (550 °C), most liquid and gas were escaped from the anvil cell because of the semi-open system although the imprint and color stains of the liquid were retained (Fig. 5).

Vitrinite samples (V31.2, V33, V34, V35.1, V37.1, V37.2, V41, and V42) appeared as dark aggregate with slightly shining reflectance. The change of appearance of the sample begun around 330 °C and ended around 550 °C during pyrolysis. Most of these vitrinite samples except one (V42) generated more or less oil-like liquid. Oil yields are generally lower than those of lipinites except two samples, E37.1 and V35.1, which yield the amounts of oil close to lipinites. The lower oil potential of the vitrinite samples than that of the lipinite samples are consistent with the previous thought and was supported by data from the diffuse reflectance infrared spectroscopy (DRIFT) analyses which show the presence of higher ratio of aliphatic to aromatic C-H stretching absorption in the studied lipinite than vitrinite samples (Machnikowska et al., 2002). Two of the vitrinite samples (V34, V33) show the spreading of small amount of medium thick and dark oil surrounding the sample while three samples (V31.2, V37.2,V41) show only the increase of sample size without visible oil flowing out of the sample and one sample (V42) show no liquid generated. The expansion of the sample size was interpreted as the retention of pyrolysates, liquid and (or) gas, in the sample. No visible gas bubbles have been observed in these vitrinite samples even for the two with significant amounts of liquid formation. The generated gas was not visible probably because of the absence of liquid phase during the gas generation. The lack of liquid phase makes the recognition of gas generation difficult. The absence of visible gas during the liquid generation indicates that the concurrent formation of gas and liquid, like that observed in lipinites, was not happen. It appears that most gas generation took place before liquid formation. The absence of gas after liquid formation implies that secondary cracking of liquid to gas may not be occurred in the temperature range of the experiments. This may be attributed to the insufficient temperature and time for secondary cracking or the evaporation of liquid out of the anvil cell before the onset of the secondary cracking. The visually observed rates of liquid formation for vitrinite samples, in general, are slower than those for lipinites.

Fusinite samples appear as fragile fibers with some shining luster. Most of fusinites are inert in response to the thermal stress during pyrolysis. Two of the samples show slight

increase of sample size, implying possibility of formation of trace amount of liquid. The presence of minor amounts of lipinite and vitrinite in the separated fusinite may account for the liquid generation.

3.2 Closed system pyrolysis

The transmission of illumination light through the sample in the closed system is not as efficient as that in semi-open system because sample was not pressed and the sample did not contact with the upper diamond face in the presence of the gasket. The visual appearance of samples, therefore, is less observable and sometimes may be even difficult to interpret. Figure 6 shows a sequence of images taken during pyrolysis for selected representative samples of lipinite (E34), vitrinite (V31.2; V35.1) and fusinite (F31.2) in the closed system pyrolysis.

The initial lipinite samples within the cell under microscope appeared as dark aggregates. The sample appearance changed continuously from 430 °C to 500 °C during pyrolysis. The temperature of the onset of oil generation is higher while that of the end is slightly lower than that in the semi-open system. The generative oils are dark with some translucent, brownish color near the edge of the sample and the fluidity ranges from “light” to “medium”; the yields of oil and gas are abundant and rank as 3 and 4. Similar to semi-open system the sample E31.2 yielded least oil. The visual reaction rates rank as “faster” fro most lipinite samples. The peak temperatures (T_{peak}) occurred in the range from 430 to 460 °C, which is slightly lower than that in the semi-open system.

Vitrinite samples appeared as dark with shining reflectance. The change of appearance begun at 450 °C and ended at 520 °C. The oil generation interval is significantly narrower than that in the semi-open system. Four out of eight vitrinite samples generated no visible oil-liquid, in contrast to one out of eight samples in the semi-open system. This suggests that pyrolysis in the semi-open system may be better to detect small amount of oil generated in vitrinite than in the closed system. The appearance of oil generation is slightly different between the semi-open and closed systems. For instance, the generative oil spreads evenly on the face of diamond in the semi-open system while the most oil tends to retain in the sample and only small amount of light oil spreads out of sample in the closed system (V35.1 in Fig. 6). For other vitrinite samples, the generation of oil was not quite visible. In some case, only the rounding of angular sample corners or slightly increase of sample size without oil flowing out of the sample was observed and the yields of oil were ranked as 1 (Table 4). Similar to that in the semi-open system, no visible gas bubbles have been observed even in the one with significant amounts of liquid formed. The visual rates of reaction for vitrinite samples are slower than those for lipinite.

Fusinite samples appear as fragile fibers with some shining luster. Most of fusinites are inert with response to the thermal stress during pyrolysis. Two of the samples show slight

increase of sample size, implying possibility of formation of trace amount of liquid.

4. Discussions

Comparison between semi-open and closed system pyrolysis reveals significantly distinct visual appearance of sample during pyrolysis. The difference may be attributed partly to the apparent optical response and partly to the difference in pyrolysis conditions including the openness of the system and the pressure. The main difference in optical response between these systems is the transparency of the samples, which in turn affect the visual appearance of oil and gas generation. This difference is small for the lipinites and fusinites but large for vitrinites (Fig. 5). Oil generated from vitrinite can not be positively recognized in closed system because it tends to retain in the sample (V34 in Fig. 6). The retention of oil in the sample in the closed system is probably due to its confined condition resulted from the increase of gas pressure in the system whereas the effective expulsion of oil observed in semi-open system may be attributed to the escape of gas from the system or to the applied stress on the samples. Gas generation in the closed system was more visible than in the semi-open system particularly for those samples generating no liquid phase. The increase of gas pressure in the sample chamber during pyrolysis under confined condition resulted in the shrinkage or the disintegration of sample, which indicates the formation of gases. The delay of the visually observed onset of oil generation may be simply due to the delay of oil expulsion because of no differential pressure on the sample in the closed system. In contrast, the stress applied to the sample in the semi-open system may enhance the oil expulsion. Although influence of the retained pyrolysates, particularly the earlier non-hydrocarbon gases, on the onset temperature in the closed system are not clear, the similarity of peak temperatures of oil generation rate in the closed and the semi-open systems (Table 5) suggests that the difference in major organic reactions occurred between the closed and semi-open systems was small. For routine application of this technique, the semi-open system is preferred because of the simplicity in performing experiments unless the gas generation is a critical issue.

The high oil yields from lipinite observed in this study is consistent with the previous thought that lipinite group contributed most liquid hydrocarbon to account for the oil-prone coal (Tissot and Welte, 1984; Snowdon, 1991; Mukhopadhyay, et al., 1991; Wilkins and George, 2002). This study confirms that there is significant variation of the oil generation potential of the different lipinites, which may be attributed to the difference in submaceral constituents in each lipinite group (Powell et al., 1991; Qin et al., 1993). For instance, the sporinite, which is one of important constituents of lipinite, has much lower oil potential than other constituents in the lipinite maceral group (Collinson et al., 1994). The observed light and high fluidity of oil appears to be in conflict with the nature of lipinites which were considered to be rich in long aliphatic chains such as wax components. The DRIFT analyses supported the presence of long aliphatic chains and naphthenic rings in the studied lipinite

(Machnikowska et al., 2002). The high fluidity of wax-bearing hydrocarbons generated from lipinites may be attributed to the liquefaction of the wax components at high experimental temperatures (> 400 °C). Alternatively, the high fluidity of the generative liquid may indeed indicate the presence of significant amounts of low molecular weight hydrocarbons. This interpretation is consistent with the observation that hydrocarbon liquid generated from some lipinite components such as liptoclarites can be relatively low in long-chain aliphatics (Stout, 1994).

Abundance of oil yields generated from two vitrinite samples (V35.1 and V37.1) was unexpected but not surprising since the oil generation potential of some vitrinite has been increasingly recognized (Stout, 1994; Wilkins and George, 2002; George and Smith, 2004). The oil-prone coals rich in vitrinite but poor in lipinite from New Zealand have been reported (Newman et al., 1997; Killops et al., 1998; Norgate et al., 1997). While the occurrence of indigenous oil-prone materials in vitrinite can not be excluded, most previous studies favor the formation of oil-prone perhydrous vitrinite during early diagenesis either through the marine-influence (George and Smith, 2004) or the impregnated with migrated oil-like materials generated from nearby lipinites (Stout, 1994). Killops et al. (1994) attributed the oil potential of New Zealand coals to the presence of desmocollinite, which may consist of dispersed sub-microscopic lipid-rich components (Liu and Taylor, 1991). However, most of the present vitrinites show “normal” or orthohydrous composition without perhydrous nature based on data determined by proximate and ultimate analyses (Table 1; Machnikowska et al., 2002). Our observed capacity of liquid generation of vitrinite samples does not correlated with their hydrogen contents, hydrogen/carbon ratio, vitrinite reflectance and other properties. It is also unlikely that the oil in these two samples was mainly generated from the lipinite as impurity in the separated vitrinite samples because the petrographic analysis reveals very low lipinite relicts (0 to 1.4 %) in these two samples (Machnikowska et al., 2002). The generation of the visually observed liquid from these vitrinites may indicate that the orthohydrous vitrinites may also generate liquid oil via unknown reaction mechanism. Collinson et al. (1994) demonstrated that periderm tissues, which would probably be included in vitrinite, are oil prone. Therefore, perhydrous nature of the vitrinite may not be necessary in order to account for oil-prone of vitrinites. Our visual observations, however, show the generative liquids from the orthohydrous vitrinite are dark and sticky and may be not similar to normal liquid hydrocarbon but more like heavy oils rich in asphaltene and NSO fractions. In contrast, the perhydrous vitrinite may generate liquid similar to normal oils .

The visual observation of oil generation from macerals also provided information useful to estimate the retention capability of oil in the individual maceral. The present experiments have demonstrated that the expulsion of oil from lipinite is as soon as it generated. The expulsion efficiency of oils generated from lipinite is high because of the high fluidity of the oil and perhaps lower retention capability of lipinite microstruture, probably formation of macroporosity after its transformation. In contrast, the expulsion of liquid from vitrinite is so

constrained that most oils were retained in the maceral causing the expansion of the maceral. The expulsion of liquid from vitrinite may be hindered by stickiness or low fluidity of the liquid and perhaps the low retention capability of its microstruture. Subsequent catagenssis at higher maturity would lead the secondary cracking into higher expulsion efficient component such gas.

5. Conclusions

The present study has demonstrated the validity of the use of *in-situ* direct visualization of organic matter during pyrolysis in the evaluation of its oil and gas generation potential. The visual observation has verified the variation of oil generation potential of three major types of macerals in coals. As previously thought, lipinite generates large amount of visible oil and gas while fusinite behaves inert during pyrolysis. The oil generation potential of the studied lipinite samples varies significantly, suggesting that oil generation potentials of different lipinites are not the same. The present study for the first time demonstrated that the retention capacity of lipinite after its transformation is low. The expulsion of oil from lipinite may not be a rate limiting step for the primary migration of in bulk coal.

Most vitrinites unexpectedly generated visible liquid, although the liquid is darker and thicker, and its yields are less than lipinites, indicating significant oil potential of the studied vitrinites. In contrast to the previous thought, the observed oil generated from the orthohydrous vitrinites implies that oil potential of vitrinite is not limited to its perhydrous nature. The expulsion of liquid hydrocarbon from vitrinite, however, is less efficient because of the high viscosity of the liquid, and probably the high retention capability of vitrinite macrostructure.

The present study shows that the major visual features pertinent to oil and gas generation in the closed system are essentially similar to those in the semi-open system, whereas the gas generation appears more noticeable in the closed system particularly for those samples generating no liquid phase. Since the semi-open experiments are much easier to perform, the DAC pyrolysis may be routinely conducted in a semi-open system if visualization of oil generation is the only concern; the performance of the closed system pyrolysis is necessary only if gas generation is the focus.

Acknowledgements

This research was supported by the Earth Sciences Sections, National Sciences Council of ROC, NSC Grant 93-2116-M002-003 to W. L. Huang.

REFERENCES

Bassett, W.A., Shen, A.H., Bucknum, M., Chou, I.M., 1993. A new diamond anvil cell for Hydrothermal studies to 2.5 GPa and from -190 to 1200 °C. Rev. Sci. Instrum. 64, 2340-2345.

Baskin, D.K., 1997. Atomic H/C ratio of kerogen as estimate of thermal maturity and organic matter conversion. American Association of Petroleum Geologist Bulletin 81, 1400 (abstract).

Bertrand, P.E., 1989. Microfacies and petroleum properties of coals as revealed by a study of North Sea Jurassic coals. International Journal of Coal Geology 13, 575-595.

Clayton, J.L., Rice, D.D., Michael, G.E., 1991. Oil-generating coals of the San Juan Basin, New Mexico and Colorado, U.S.A. Organic Geochemistry 17, 735-742.

Collinson, M.E., van Bergen, P.F., Scott, A.C., de Leeuw, J.W., 1994. The oil generating potential of plants from coal and coal-bearing strata through time: a review with new evidence from Carboniferous plants. In: Scott, A.C., Fleet, A.J. (Eds.), Coal and Coal-Bearing Strata as Oil-Prone Source Rocks? Geological Society Special Publication 77, pp. 31-70.

Durand, B., Paratte, M., 1983. Oil potential of coals: a geochemical approach. In Petroleum Geochemistry and Exploration of Europe, ed. J. Brooks. Geological Society (Special Publication)12, 255-265. Blackwell Scientific, Oxford.

George, S.C., Smith, J.W., 2004. Variability of molecular source and thermal maturity indicators in a marine-influenced coal seam: the Greta Seam, Sydney basin. Abstracts of the 21th Annual Meeting of Society for Organic Geochemistry 21, 77.

Huang, D., Qin, K., Wang, T., Zhou, X. et al., 1997. Formation and Mechanism of Oil from Coal. Petroleum Industry Press, Beijing, 443pp.

Huang, W.L., 1996. A new pyrolysis technique using diamond anvil cell: In-situ visualization of kerogen transformation. Organic Geochemistry 24, 95-107.

Huang, W.L., Bassett, W.A. and Wu, T.C., 1994. Dehydration and hydration of montmorillonite at elevated temperatures and pressures monitored using synchrotron radiation. Am. Mineralogists 79, 683-691.

Huang, W.L., Otten, G.A., 1998. Oil generation kinetics determined by DAC-FS/IR pyrolysis: technique development and preliminary results. Organic Geochemistry 29, 1119-1137.

Hunt, J.H., 1991. Generation of gas and oil from coal and other terrestrial organic matter. Organic Geochemistry 17,673-680.

Hunt, J.M., 1996. Petroleum Geochemistry and Geology, 2nd Edtion. Freeman, New York.

Killops, S.D., Funnell, R.H., Suggate, R.P., Sykes, R., Peters, K.E., Walters, C., Woolhouse, A.D., Weston, R.J., Boudou, J.P., 1998. Predicting generation and expulsion of paraffinic oil from vitrinite-rich coals. Organic Geochemistry, 29, 1-21.

Killops, S.D.,Woolhouse, A.D., Weston, R.J., Cook, R.A., 1994. A geochemical appraisal of oil generation in Taranaki Basin, New Zealand. AAGP Bulletin 78, 1560-1585.

Land, D.H., Jones, C.M., 1987. Coal geology and exploration of part of the Tertiary Kutei Basin in East Kalimantan, Indonesia. In: Scott, A.C. (Ed.), Coal and Coal-Bearing Strata: Recent Advance. Geol. Soc. Spec. Publ. 32, 235-255.

Law, B.E., and Rice, D.D.(ed.), 1993. Hydrocarbons from coal. AAGP Studies in Geology, 38.

Lewan, M.D., 1997. Experiments on the role of water in petroleum formation. Geochim. Cosmochim. Acta 61, 3691-3723.

Liu, S.L., Taylor, G.H., 1991. TEM observation on Type III kerogen, with special reference to coal as a source rock. Journal of Southeast Asian Earth Sciences 5, 43-52.

Machnikowska, H., Krzton, A., Machnikowski, J., 2002. The characterization of coal macerals by diffuse reflectance infrared spectroscopy. Fuel 81, 245-252.

Miknis, F.P., Sullivan, M., Bartuska, V.J., Maciel, G.E., 1981. Cross-polarization magic-angle spinning 13C NMR spectra of coals of varying rank. Org. Geochem. 3, 19-28.

Miknis, F.P., Netzel, D.A., Surdam, R.C., 1996. NMR determination of carbon aromatization during hydrous pyrolysis of coals from the Mesaverde Group, Greater Green River Basin. Energy & Fuels 10, 3-9.

Moore, P.S., Burns, B.J., Emmett, J.K., Guthrie, D.A., 1992. Integrated source, maturation and migration analysis, Gippsland Basin, Australia. Australian Petroleum Exploration Association Journal 32, 313-324.

Mukhopadhyay, P.K., Hatcher, P.G., Calder, J.H., 1991. Hydrocarbon generation from deltaic and intermontane fluviodeltaic coal and coaly shale from the Tertiary of Texas and Carboniferous of Nova Scotia. Organic Geochemistry 17, 765-783.

Newman, J., Price, L.C., Johnston, J.H., 1997. Hydrocarbon source potential and maturation in Eocene New Zealand vitrinite-rich coals. Journal of Petroleum Geology 20, 137-163.

Norgate, C.M., Boreham, C.J., Kamp, P.J.J., Newman, J., 1997. Relationship between hydrocarbon generation, coal type and rank for Middle Eocene coals, Buller Coalfield, New Zealand. Journal of Petroleum Geology 20, 427-458.

Pepper, A.S., Corvi, P.J., 1995. Simple kinetic models of petroleum formation. III. Modeling an open system. Marine and Petroleum Geology 12, 417-452.

Powell, T.G., and Boreham, C.J., 1991. Petroleum generation and source rock assessment in terrigenous sequences: an update. Australian Petroleum Exploration Association Journal 29, 114-129.

Qin, K.Z., Chen, D.Y., Li, Z.G., 1991. A new method to estimate the oil and gas potentials of coals and kerogens by solid state ^{13}C NMR spectroscopy. Organic Geochemistry 17, 865-872.

Qin, K.Z., Huang, D.F., Li, L.Y., Guo, S.H., 1993. Oil and gas potential of macerals as viewd by ^{13}C NMR spectroscopy. In Organic Geochemistry, Poster Sessions from the 16th International Meeting on Organic Geochemistry, ed. K. Oygard, pp.758-762. Falch Hurtigtrykk, Oslo.

Scott, A.C., Fleet, A.J., 1994. Coal and coal-bearing strata as oil-prone source rocks? Geological Society Special Publication 77.

Smith, G.C., Cook, A.C., 1984. Petroleum occurrence in the Gippsland Basin and its relationship to rank and organic matter type. Australian Petroleum Exploration Association Journal 24, 196-216.

Snowdon, L.R., 1991. Oil from type III organic matter: resinite revisited. Organic Geochemistry 17, 734-747.

Stankiewicz, B.A., Kruge, M.A., Mastalerz, M., 1996. A geochemical study from a Miocene lignite and an Eocene bituminous coal, Indonesia. Organic Geochemistry 24, 531-545.

Stout, S.A., 1994. Chemical heterogeneity among adjacent coal microlithotypes-implications for oil generation and primary migration from humic coal. In: Scott, A.C., Fleet, A.J. (Eds.), Coal and Coal-bearing Strata as Oil-prone Source Rocks? Geological Society Special Punlication 77, pp.93-106.

Tissot, B.P., Welte, D.H., 1984. Petroleum Formation and Occurrence, 2nd ed., 699 pp. Springer, New York.

Weng, R.F., Huang, W.L., Kuo, C.L., Inan S., 2003. Characterization of oil generation and expulsion from coals and source rocks using diamond anvil cell pyrolysis. Organic Geochemistry 34, 771-787.

Wilkins, R.W.T., George, S.C., 2002. Coal as a source rock for oil. Int. J. Coal Geol. 50, 317-361.

Figure Captions

Figure 1. The elemental analysis of the maceral samples on van Krevan diagram (Data from Machnikowska et al., 2002).

Figure 2. Experimental setup for diamond anvil cell pyrolysis technique.

Figure 3. Schematic diagram of diamond anvil cell for closed system pyrolysis.

Figure 4. Semi-quantitative analysis of liquid yields: (a) cumulative curves, (b) rate curves; the T_{peak} was determined by the peak temperature.

.

Figure 5. Images of four representative samples monitored in-situ during pyrolysis in semi-open system; the images for the corresponding stages.

Figure 6. Images of four representative samples monitored in-situ during pyrolysis in closed system; the images for the corresponding stages are

Figure 7. Comparison of temperature (T_{peak}) of maximum rate of oil generation in semi-open and closed system.

Table Captions

Table 1. Proximate and ultimate analysis of macerals (Machnikowska *et al*., 2002).

Table 2. Petrographic analysis (% V/V, mmf) and vitrinite reflectance (%) of macerals in the studied coals (Machnikowska *et al*.,2002).

Table 3. Summary of visual characteristics of maceral concentrates during pyrolysis in semi-open system.

Table 4. Summary of visual characteristics of maceral concentrates during pyrolysis in closed system.

Table 5. The temperatures of oil and gas generation during pyrolysis in open and closed systems

附錄三　計劃主持人近五年著作目錄

(A) SCI 論文

1. Lee, W. J., Huang, W. L., Wyllie, P. J., 2000. Carbonate-rich melts in the mantle modeled in the system CaO-MgO-SiO_2-CO_2 at 2.7 GPa, Contr. Mineralogy Petrology 38, 199-213. (NSC 88-2119-M-002-005). (SCI)
2. Huang, W.L., Otten, G.A., 2001. Cracking kinetics of crude oil and alkanes determined by diamond anvil cell-fluorescence spectroscopy pyrolysis: technique development and preliminary results. Organic Geochemistry 32, 817-830. (NSC 89-2116-M-002-055). (SCI)
3. Huang, W.L., 2002. Nanoquartz: synthesis in neutral solutions at high pressure. Journal of Crystal Growth 244, 178-182. (NSC 89-2119-M-002-055) (SCI)
4. Weng, R.F., Huang, W.L., Kuo, C.L., Inan, S., 2003. Characterization of oil generation and expulsion from coals and source rocks using diamond anvil cell pyrolysis. Organic Geochemistry 34, 771-787. (NSC 88-2119-M-002-005) (SCI)
5. Huang, W.L., 2003. The nucleation and growth of polycrystalline quartz: Pressure effect from 0.05 to 3 GPa. European Journ. Mineralogy 15, 843-853. (NSC 90-2116-M-002-008) (SCI)
6. Huang, W.L., 2003. Synthetic polycrystalline aragonite to calcite transformation kinetics: experiments at pressures close to equilibrium boundary. Mineralogy and Petrology 79, 243-258. 91. (NSC 90-2116-M-002-008) (SCI)
7. Cheng, A.L., Huang, W.L., 2004. Selective adsorption of hydrocarbon gases on clays and organic matter. Organic Geochemistry V35/4, 413-423. (89-2119-M-002-055) (SCI)
8. Lin, S.J., Huang, W.L., 2004. Polycrystalline calcite to aragonite transformation kinetics: experiments in Synthetic Systems. Contr. Mineral. Petrology 147, 604-614. (NSC 91-2116-M-002-028) (SCI)
9. Shen, P.Y., Hwang, S.L., Chu, H.T., Yui, T.F., Pan, C.N., Huang, W.L., 2005. On the transformation pathways of α-PbO_2-type TiO_2 at the twin boundary of rutile bicrystals and the origin of rutile bicrystals .European Journal of Mineralogy. (SCI) (in press).
10. Shen, J.C., Huang, W.L., 2005. Biomarker distribution in coals, source rocks and oil in Taiwan with newly defined maturity parameters. International Journal of Coal Geology. (submitted)
11. Pan, C.N., Shen, P.Y., Huang, W.L., Hwang, S.L., Yui, T.F., Chu, H.T., 2005. High temperature-pressure synthesis of Ti-doped tohdite and corundum from hydrous Al_2O_3-TiO_2 gel: implications for natural occurrence and engineering applications. Contr. Mineral. Petrology. (submitted)

12. Su, K.W., Huang, W.L., 2005. Generation of hydrocarbon gases and CO_2 from a humic coal: Experimental study on the effect of water, minerals and transition-metals. Organic Geochemistry. (in revision)

(B)研討會論文

1. Huang, W.L., 1999. Oil and gas generation kinetics monitored by visualization, fluorescence and infrared spectroscope in diamond anvil cell. 1999 Annual Meeting of Geological Society of China, p.177.
2. Sempere, J.C., Curry, D.J., Hill, R.J., Huang W.L., 1999. Prediction of the composition of hydrocarbons generated from oil-prone coals in the Gippsland basin. AAPG Annual Meeting, Dallas.
3. Weng, R.F., Huang, W.L., 2001. Oil generation and expulsion simulated using diamond anvil cell: Application of a new pyrolysis technique. 2001 Annual Meeting of Geological Society of China, Taipei, March, 2001, Abstract, p.323-324. (NSC 88-2119-M-002-005)
4. Lin, S.J., Huang, W.L., 2001. Transformation kinetics of synthetic polycrystalline calcite to aragonite. 2001 Annual Meeting of Geological Society of China, Taipei, March, 2001, Abstract, p.317-319. (NSC 88-2119-M-002-005)
5. Huang, W.L., 2001. A multi-sample, programmed-heating, and rapid-quench apparatus for confined or MSSV pyrolysis. 20th International Meeting on Orgaic Geochemistry, Nancy, France, Abstract v.2, p.239-240.
6. Huang, W.L., 2001. The nucleation and growth of polycrystalline quartz: pressure effect up to 3 GPa. 2001 Joint Geosciences Assembly, Taipei, September, 2001, Program Proceeding , p.25-26. (NSC 89-2116-M-002-055)
7. Cheng, A.L., Huang, W.L., 2001. Absorption of natural gas during migration: an experimental study. 2001 Annual Meeting of Geological Society of China, Taipei, March, 2001, Abstract, p.320-322. (NSC 89-2116-M-002-055)
8. Huang, W.L., 2002. Retrogade metamorphic reaction kinetics of carbonate rocks Lo and Chien Retirement Conf., 2002 June 7, Taipei. (NSC 90-2116-M-002-008)
9. Huang, W.L., 2002. Nanoquartz: synthesis in neutral solution at high pressures. ICSTR Conference, East Brunswick, NJ, USA. (NSC 89-2116-M-002-055)
10. Weng, R.F., Huang, W.L., Kuo, C.L., Inan, S., 2002. Oil generation and expulsion from coals and source rocks using diamond anvil cell pyrolysis. "Emerging Concepts in Organic Petrology & Geochemistry" -the 2002 Joint Meeting of The Canadian Society for Coal Science and Organic Petrology and The Society for Organic Petrology. (accepted). (NSC 88-2119-M-002-005)
11. Cheng, A.L., Huang, W.L. 2002. Selective Adsorption of Hydrocarbon Gases on Clays

and Organic Matter: An Experimental Study. "Emerging Concepts in Organic Petrology & Geochemistry" -the 2002 Joint Meeting of The Canadian Society for Coal Science and Organic Petrology and The Society for Organic Petrology. (accepted) (NSC 89-2116-M-002-055)

12. Steel, K.M., Castro Diaz, M., Patrick, J.W., Huang, W.L., Snape, C.E., 2003. Understanding the viscoelastic behaviour of coal during pyrolysis using rheometry, H-NMR and visual techniques. 12th International Conference on Coal Science, Australia.
13. Huang, W.L., 2003. Influence of pressure on gas generation and vitrinite maturation under confined pressure pyrolysis. 21st International Meeting on Organic Geochemistry. Krakow, Poland.
14. Su, K.H., Huang, W.L., 2004. The generation of hydrocarbon gases and CO_2 from a humic coal: Experimental study on the effect of mineral-water reactions.2004 Gordon Research Conference.
15. Huang, W.L., 2004. Dynamic of methane hydrate in pore space: micro-visualization in a diamond anvil cell. International Workshop on Gas Hydrate Exploration and Exploitation Conference Proceedings, 43-47.

行政院國家科學委員會補助專題研究計畫
出席國際會議心得報告

※※※※※※※※※※※※※※※※※※※※※※※※※※

※　　　　　　　　　　　　　　　　　　　　　　　　※

※　有機物、礦物及水在深埋或隱沒沉積物中交互作　※

※　　　　　　　　用之實驗研究　　　　　　　　　※

※　　　　　　　　　　　　　　　　　　　　　　　　※

※※※※※※※※※※※※※※※※※※※※※※※※※※

計畫類別：☑個別型計畫　　□整合型計畫

計畫編號：NSC　93－2116－M－002－003

執行期間：　93 年　8 月　1 日至　94 年　7　月　31　日

計畫主持人：黃武良(wlhuang@ntu.edu.tw)

本出席國際會議心得報告包括以下應繳交之附件：

☑會議發表講稿一份

執行單位：國立台灣大學地質科學系

中　華　民　國　94　年　7　月　8 日

行政院國家科學委員會專題研究計畫
出席國際會議心得報告

有機物、礦物及水在深埋或隱沒沉積物中交互作用之實驗研究

計畫編號：NSC 93-2116-M-002-003
執行期限：93 年 8 月 1 日至 94 年 7 月 31 日
主持人：黃武良　國立台灣大學地質科學系

出席 2005 年 12th ISATT國際會議報告

(2005)七月三日至六日在 Sydney, Australia 舉行

The conference and personal participation (會議簡介及參加過程**)**

The 12th International Conference for international study association on teachers and teaching (ISATT conference) was held in Sydney, Australia on July 3 to July 6, 2005. The Conference was sponsored by International Study Association based in the United Kingdom. The conference was held every other year in different countries. The 12th conference in 2005 was hosted by Australia.

The themes of the conference include (1) connections, (2) community, (3) creativity and (4) competence –encapsulate the important challenges in research and education today for our changing, complex and interdependent world. The breath and depth of scholarship and experience represented by the participants at this international conference positioned us well for addressing these themes.

The programs of the conferences include four Keynote Speeches addressed by four outstanding scholars from Belgium, USA, New Zealand and Australia, fifty sessions of paper presentation, two symposiums and one workshop. In the conference, I have attended the many paper presentations and one symposium which are related to my research area. In order to be viewed as an active participant, I have presented a 30 minutes talk entitled “Improving college students understanding geosciences phenomena through visualization”.

The observations in the conference (與會心得)

The conference gathers more than 150 scholars with a variety of backgrounds from more than 15 countries worldwide. This is one of the most important conferences which address the current issues in teaching and research in education. The conference presented the change and challenge of our new Century has faced. Through the presentations and discussions, I have learned and gathered important information which is very useful to my current research and teaching. My presentation of our innovative research results on the Diamond anvil Cell (see attached) as a visualization tool to understand geochemical reactions at harsh geological conditions has been well received and of interest to many audiences. The comments and questions during the discussion of my presentation received in the conference have significantly improved my research quality and provided new insight in my research area. In addition, I have met and acquainted some scientists, educators and teachers from different countries in the conference.

Suggestions (建議)

In the conference, there is a focus on the perspectives and direction of education. A consensus that our future life in a global village depends on the quality and diversity of each country's communities of learners has been reached. As a university faculty, I feel from the learning in the conference that teaching is as important as doing research. Our current emphasis on the research but ignorance of the quality of teaching in Taiwanese academia may lead to an imbalanced knowledge society. I recommend the educators in our country should take a serious consideration about our future direction in higher education. In my personal research area, I suggested that our experiments conducted for our research can be as good as teaching tools for college students. Learning from experiments is the best way to understand complicate geological phenomena.

附件

會議發表講稿一份

Improving college students' understanding of geoscience's phenomena through visualization using visual aids

Wuu-Liang Huang and Shwu-yong Huang

National Taiwan University
Taipei, Taiwan

Geosciences Phenomena

Some of these phenomena, in particular, the geochemical reactions, are unable to observe because

- they occurred in the past
- they occurred at subsurface or deep sea.

Experimental simulations

Most experimental simulations are conducted at high pressure and non-ambient temperature and hard to visualize

Objectives of this study

I. Design experiments to allow students to visualize geochemical reactions occurred at harsh geological conditions

II. Investigate students' learning behavior with and without the visual aids

Diamond Anvil Cell as a Teaching Tool

Examples

(I) Oil and gas generation at subsurface

(2) Gas hydrate formation and dissociation at sea bottom

Diamond Anvil Cell

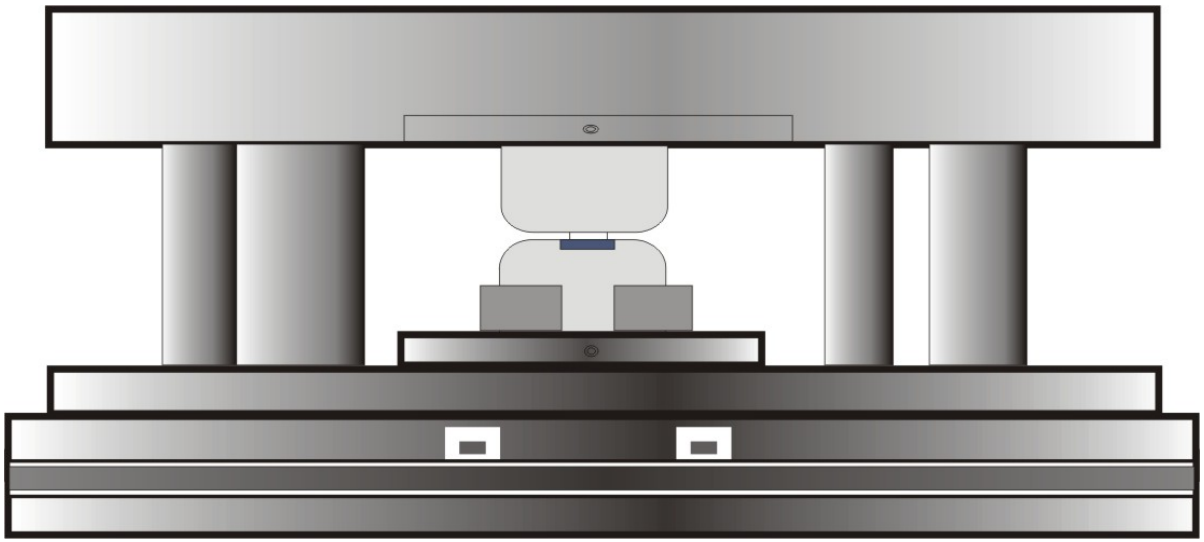

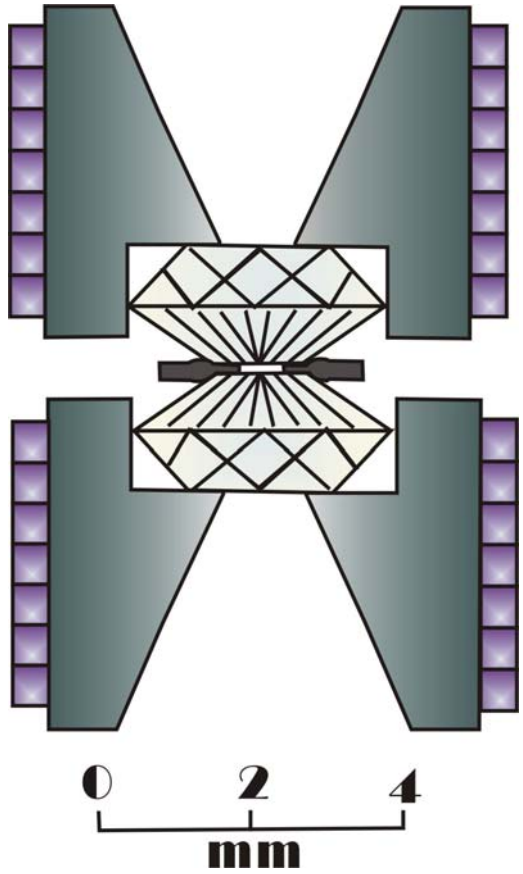

Other equipment with optical window, e.g. with sapphire window, may work as well

Diamond Anvil Cell

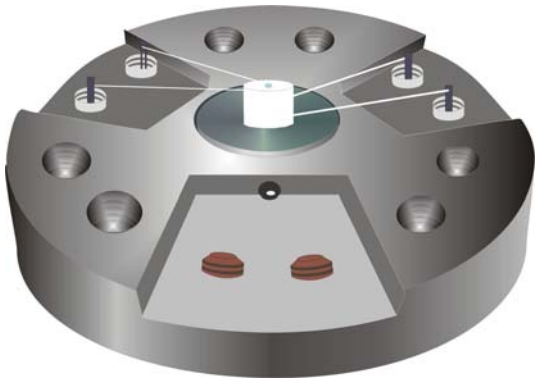

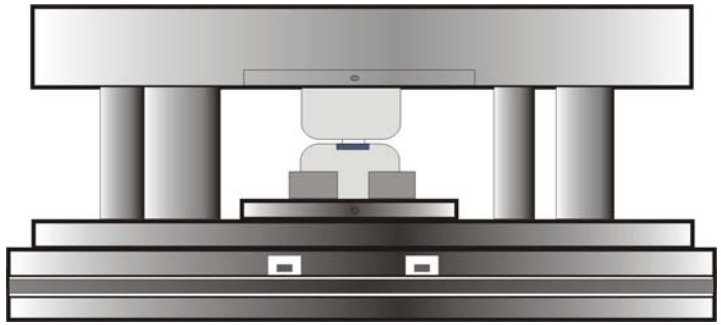

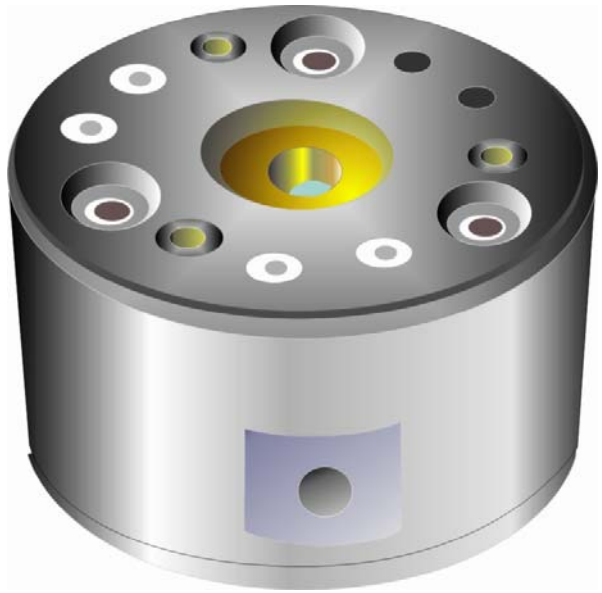

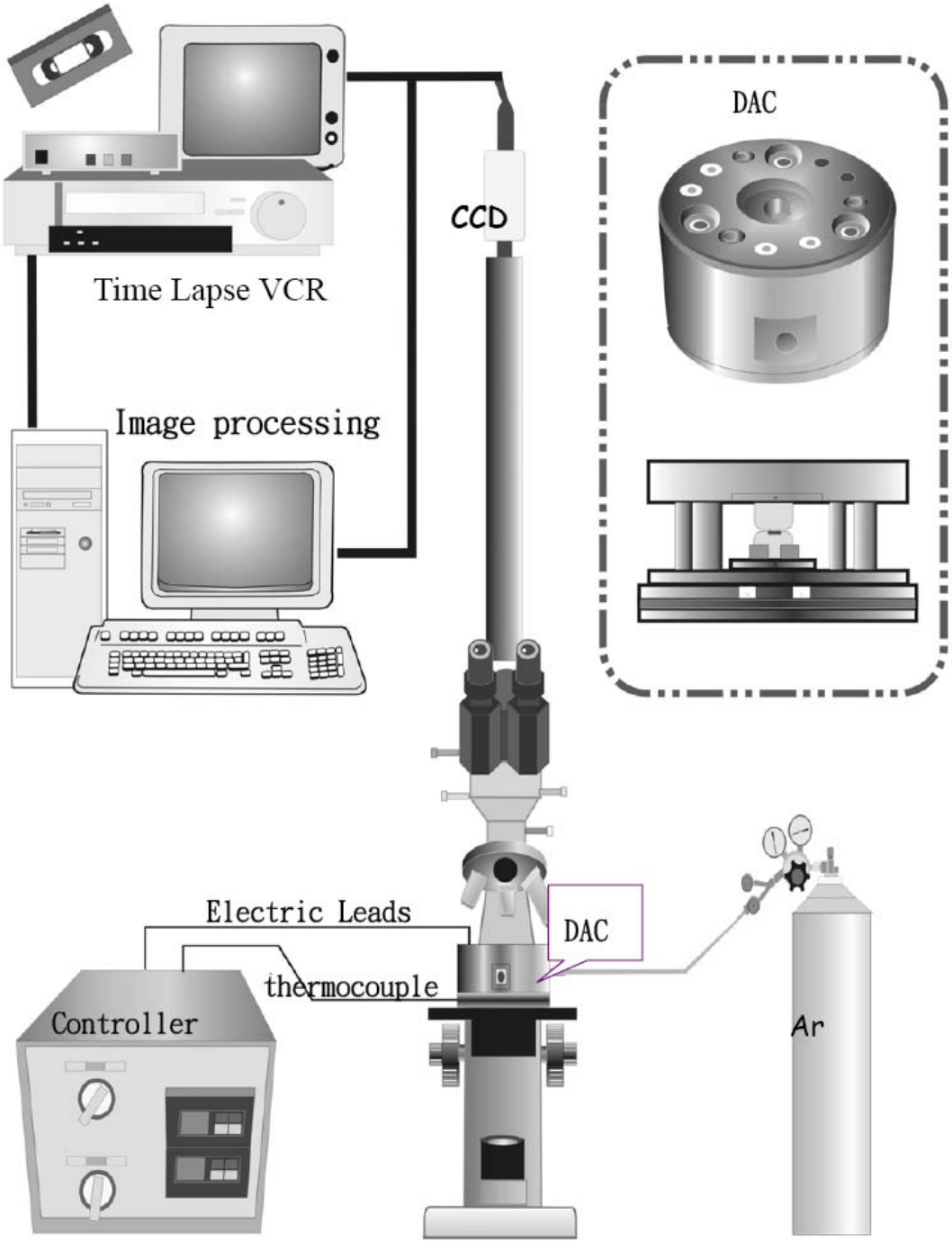
DAC
CCD
Time Lapse VCR
Image processing
Electric Leads
DAC
thermocouple
Controller
Ar

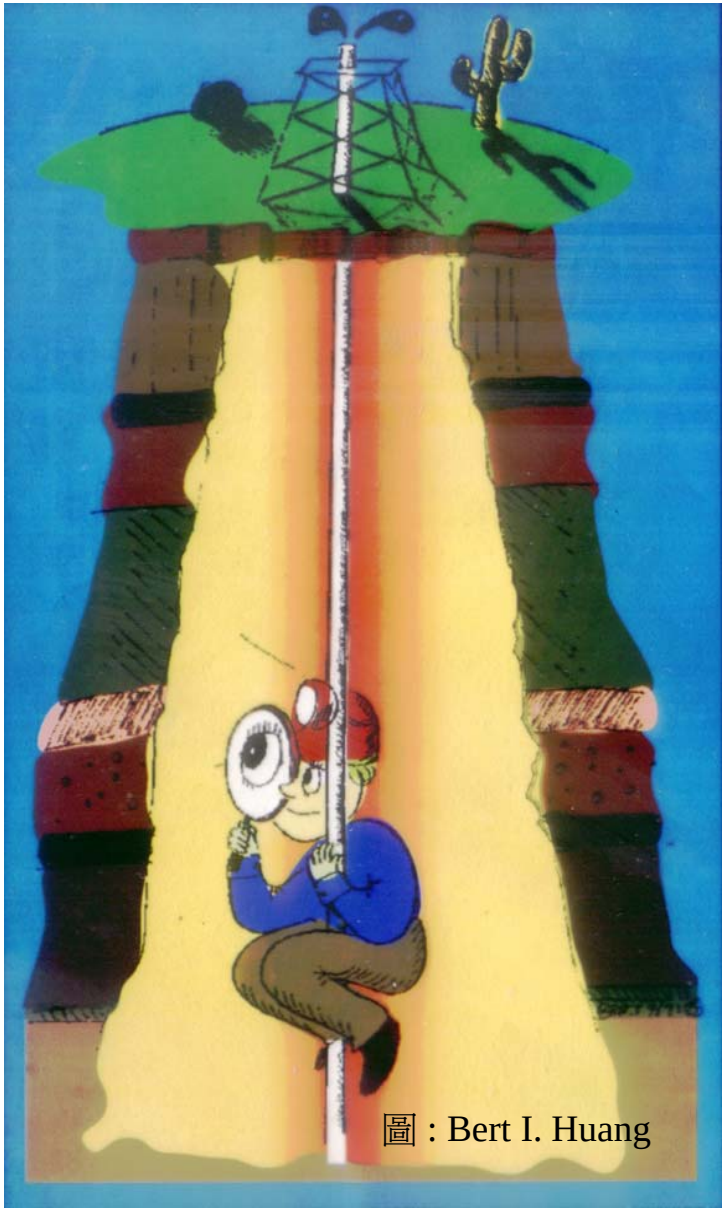

Seeing is believing

Example I

Oil and gas generation at subsurface

Visualization

How were oil and gas generated from solid organic matter (kerogen or coal) in burial sediments ?

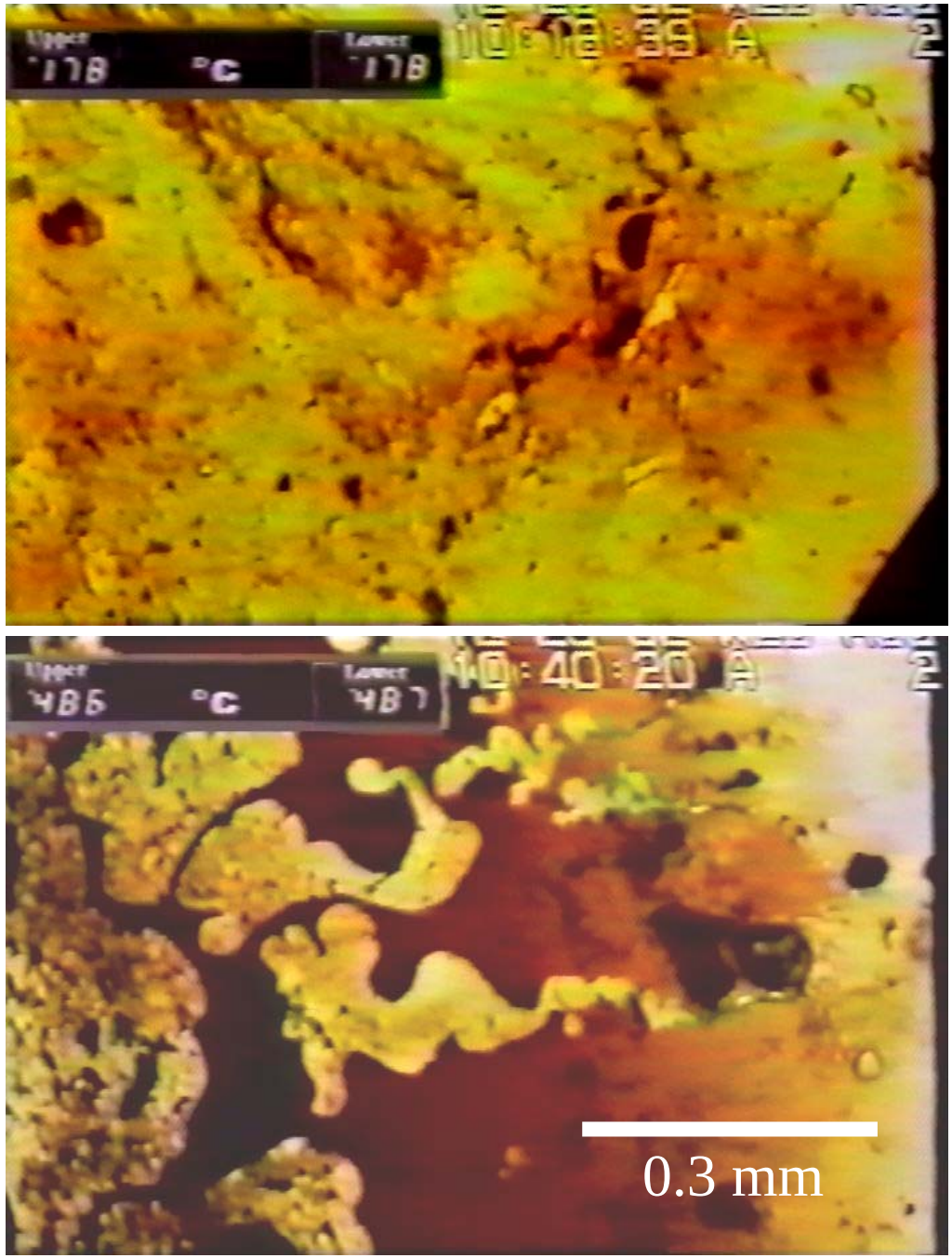
0.3 mm

Visualization of oil generation and expulsion for four coals

Table

	Initial	peak	end
Coal 2			
Coal D			
Coal 3			
Coal 31	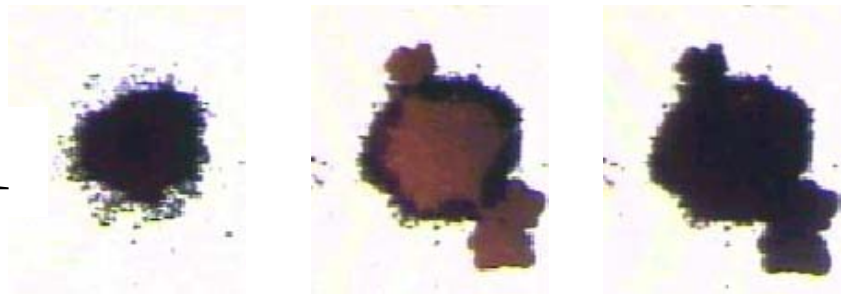		

Weng et al., 2003

What can students learn from visualization ?

1. **How were oil and gas generated from source rocks (or coals) ?**

   (A video worths a thousand words)

2. **Which source rocks (or coals) generated oil and which generated gas ?**

   (Not all source rocks are equal)

What can students learn from visualization

3. When and how much oil and gas were generated ?

(Predict the timing and potential of oil and gas for different source rocks)

4. How does oil and gas migrate within the rocks ?

(Measure oil and gas expulsion efficiency)

Example II

Gas hydrate formation and dissociation at sea bottom

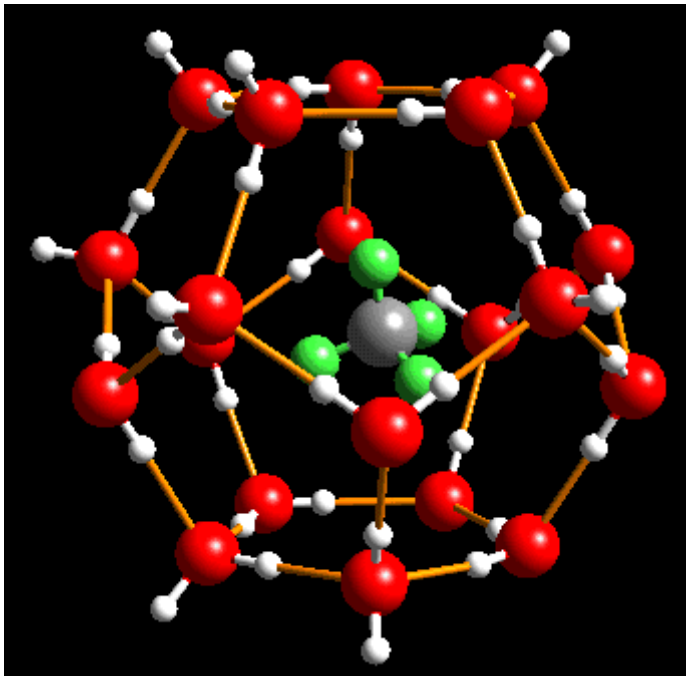

Adapted from LLNL

Methane hydrate

$CH_4 . 6H_2O$

Ice-like structure

Flammable Ice

Natural Gas Hydrate in sediments

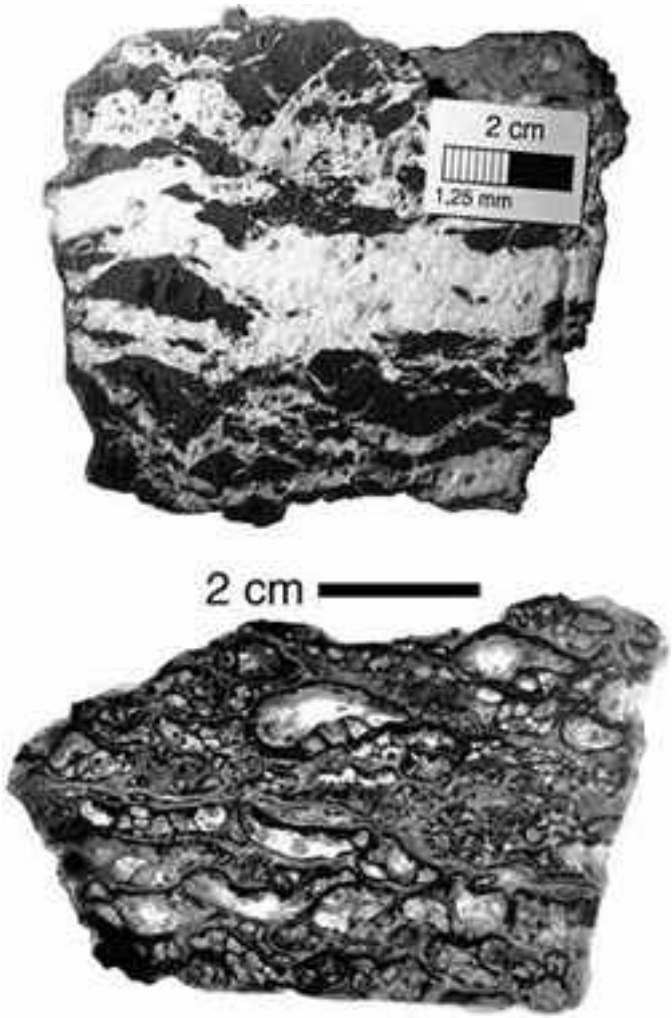

Adapted from IFM-GEOMAR

Flammable Ice

Adapted from Osaka Gas Co.

Distributions of natural gas hydrate

(potential natural gas resources)

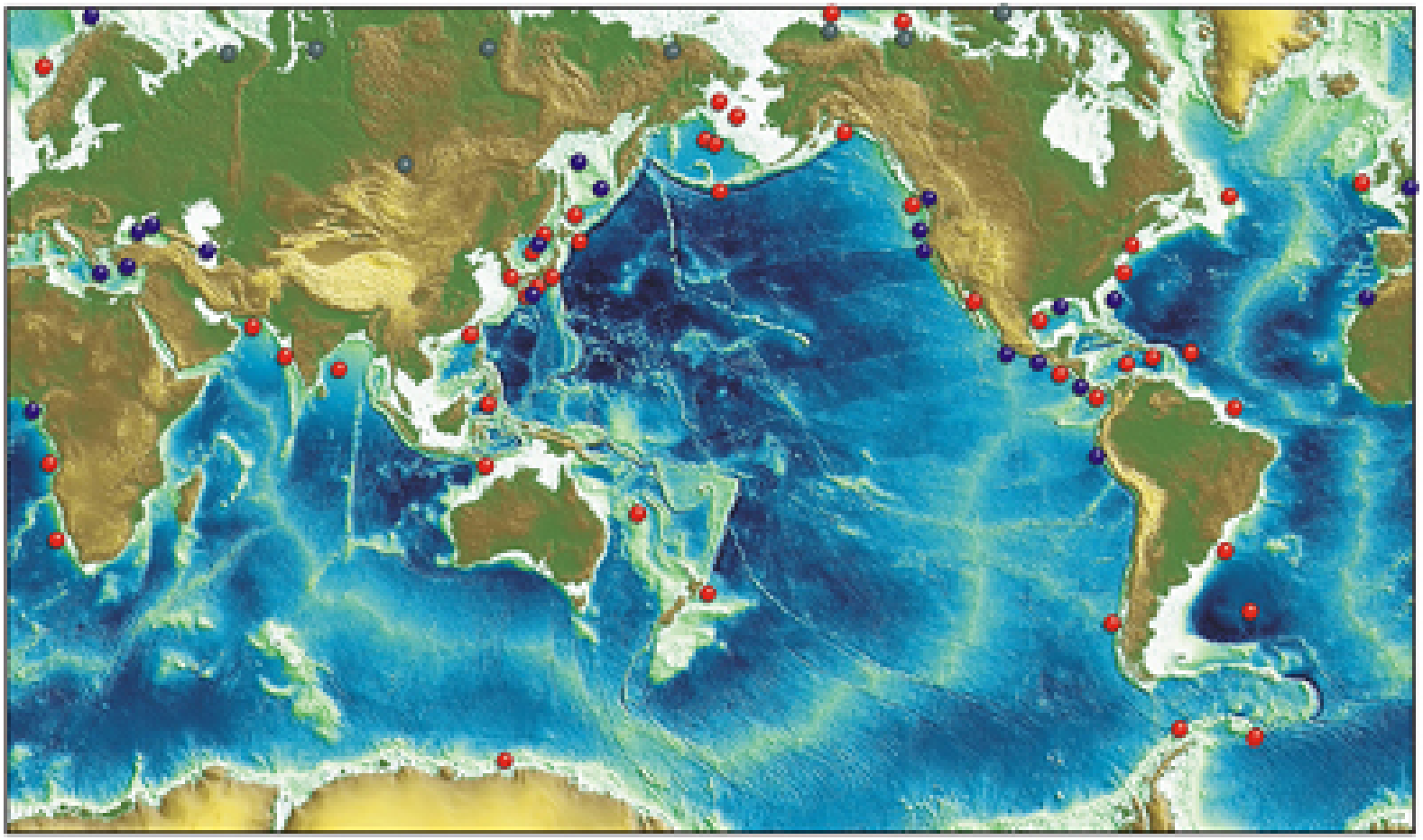

The Leibniz Institute of Marine Sciences at the University of Kiel (IFM-GEOMAR)

Phase diagram

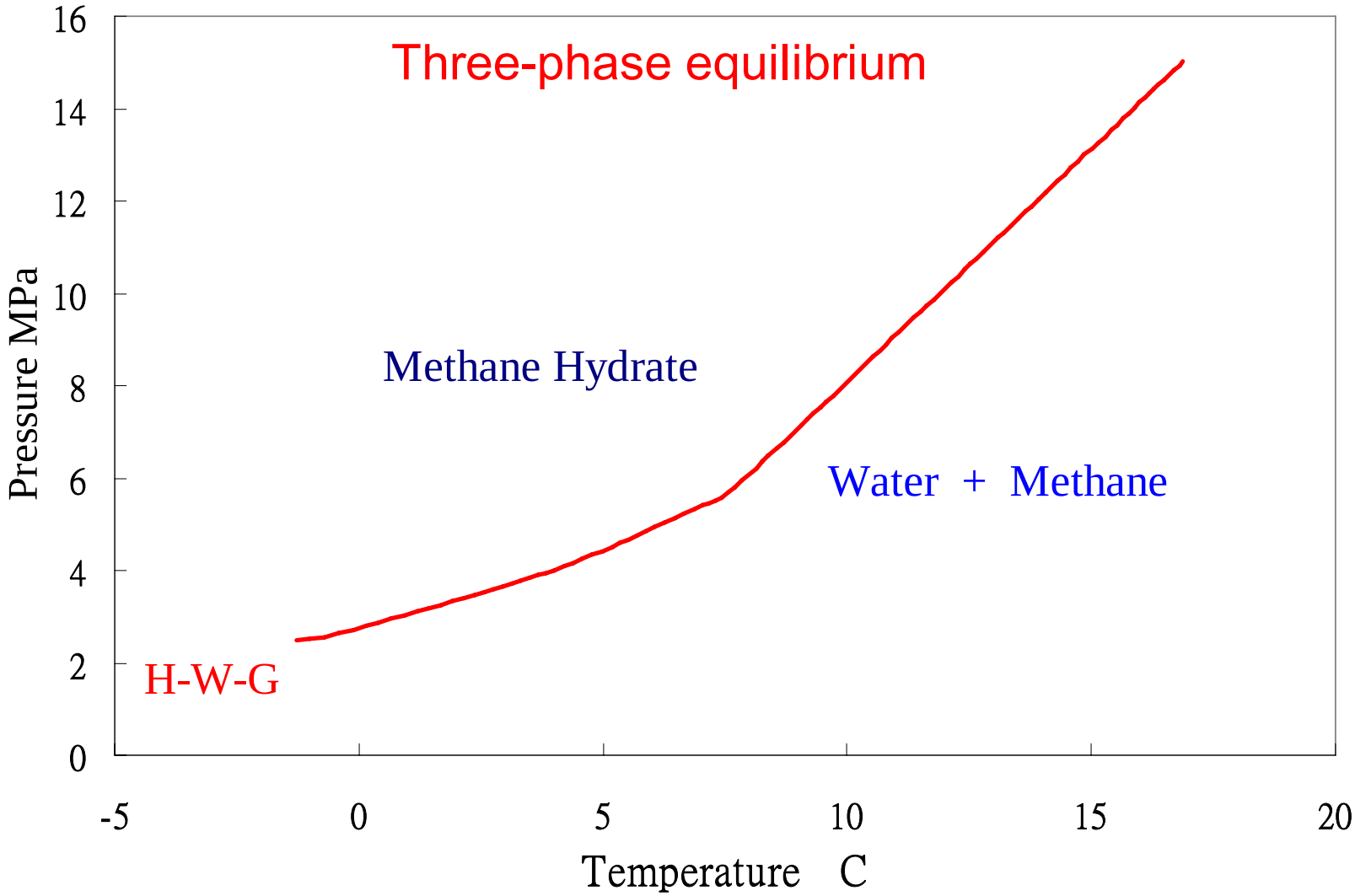

Gas hydrate formation and dissociation at sea bottom

Visualization

- What does methane hydrate look like within the pore space of sediments ?

- How does methane hydrate dissociate at sea bottom ?

Diamond Anvil Cell

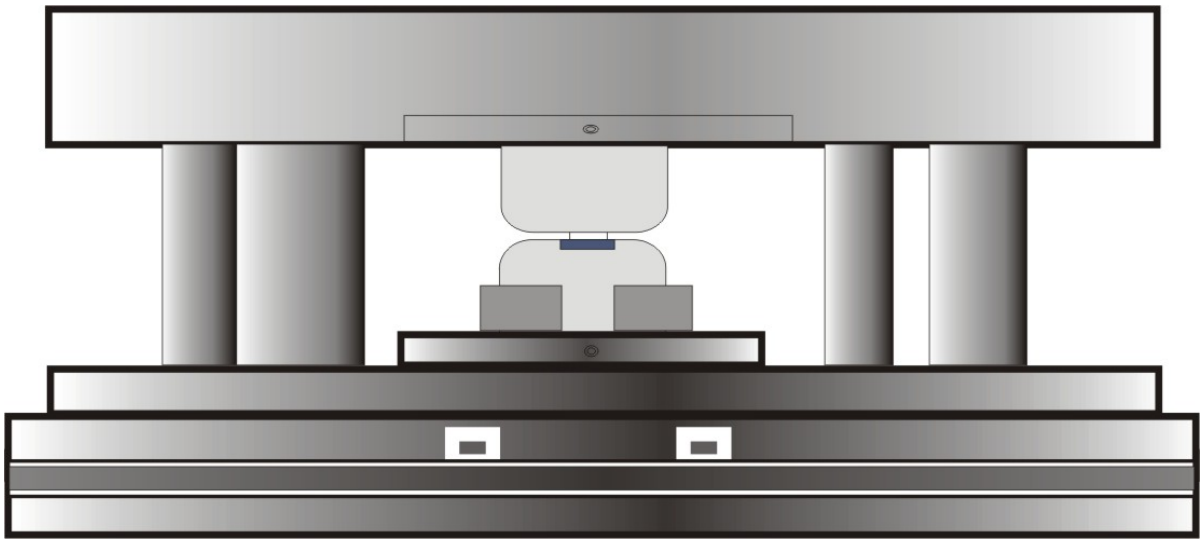

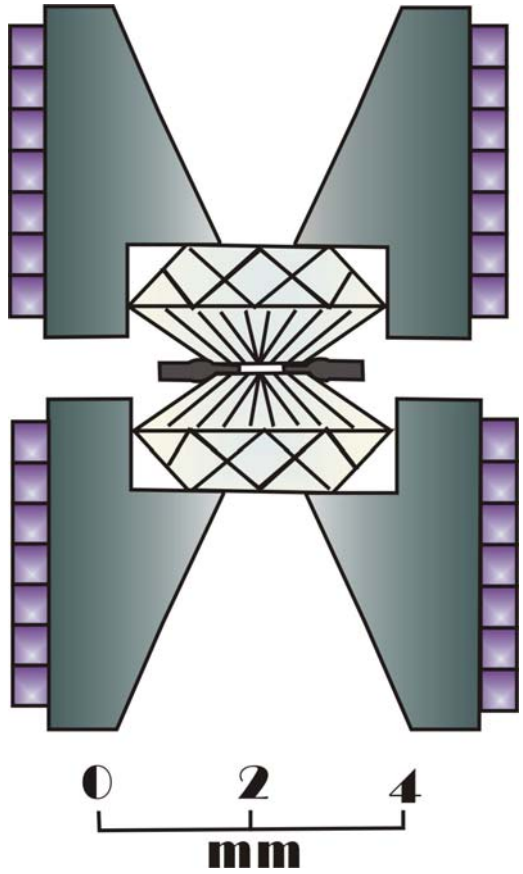

Water + methane

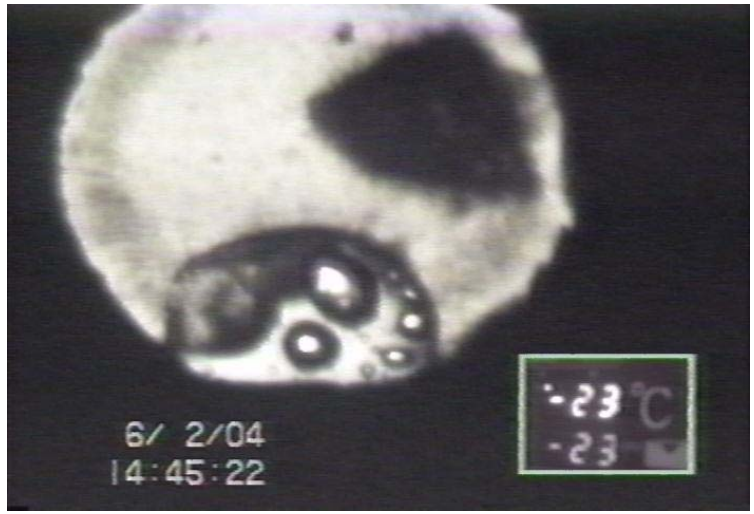

Hydrate formation

Hydrate recrystallization

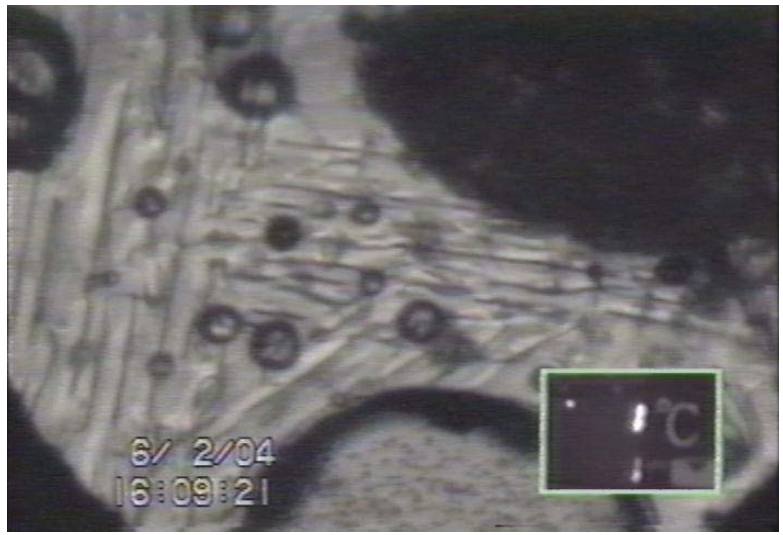

Hydrate dissociation

Diffusion control of bubble formation

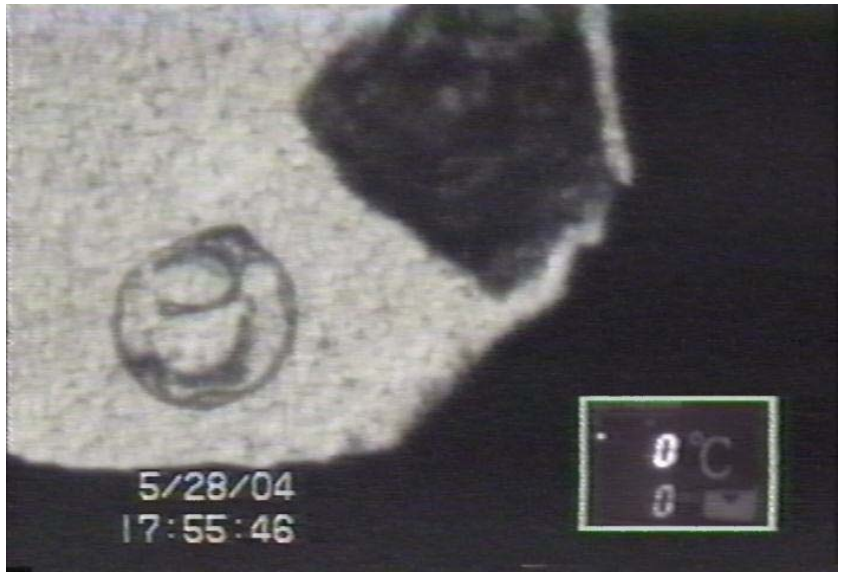

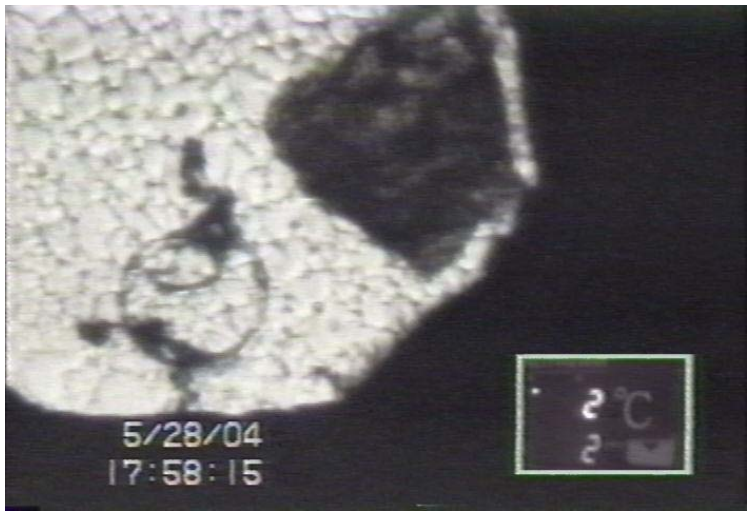

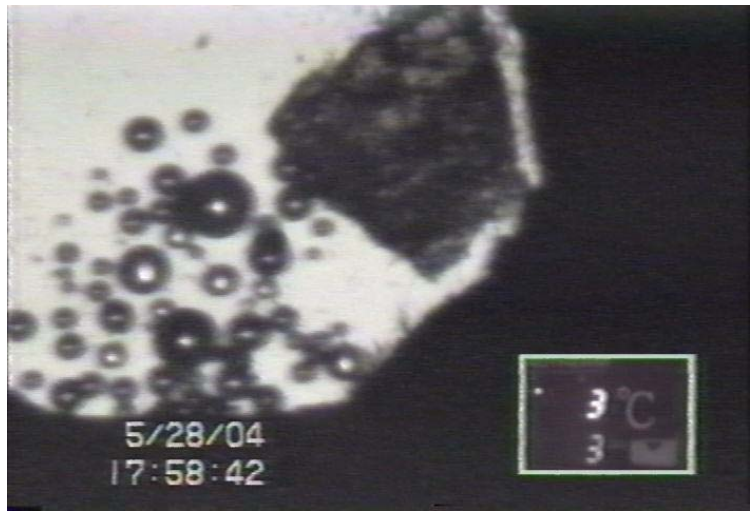

What can students learn from visualization ?

1. What do hydrate crystals look like (morphology, size and dynamics) ?

2. How fast do the hydrate crystals nucleate and grow ?

(nucleation retards hydrate formation)

What can students learn from visualization ?

3. The restless of methane gas hydrate crystals. (solid-state re-crystallization or annealing)

4. The dissociation temperature (i.e. melting point) of gas hydrate depends on pressure.

Students' learning behavior with the visual aids

- Observations from two classes of basic geoscience course

College Students				
Year	2004		2005	
the visual aid	No		Yes	
Major	Geoscience	Non-geoscience	Geoscience	Non-geoscience
Number of students	about 45	about 55	about 40	about 60

Student group in 2004 is different from that in 2005

Students' response with the visual aid

- Students are more interested in the topics
- Students ask more questions and discuss about what they see
- Students answer better the problems in the class examination
- The visual aid appears more helpful to non-geoscience students

CONCLUSION (I)

- **Diamond Anvil Cell can be a promising visual aid for students to study geological phenomena**
- **We have demonstrated with two examples:**

  - how petroleum was generated from coals or organic-rich rocks at elevated temperatures and pressures

  - how gas hydrate behaves within micro pores in sea bottom sediments

CONCLUSIONS (II)

- Preliminary study shows that the visual aids improved the students' understanding of these geological processes
- Many other experiments under harsh conditions can be conducted to produce similar visual aids to improve students' understanding

Future Study

- Quantify and compare students' learning behavior with and without the visual aids
- Design other experiments to produce similar visual aids for other geoscience's phenomena

Seeing is believing”is particularly true for students who are beginners in a new subject area. Geoscience teachers face challenge to present some geoscience phenomena through visualisation because these phenomena commonly occur only under harsh conditions and are difficult to observe. The objective of this project is to design innovative experiments using an optical window which enables students to visualize or record the processes of the phenomena. The present study demonstrates this technique using two examples. In the first example, students learn, via the recorded video, how petroleum was generated from coals or a variety of organic-rich rocks during thermal maturation at elevated temperatures and pressures, which normally took place at Earth's subsurface in millions of years. Next, we focus on methane hydrate, which is a naturally formed ice-like phase consisting of methane and water and is considered as an important source of natural gas in the future. In this example, students can visualize the processes showing the crystallization and dissociation of methane hydrate, which took place only in sediments below sea bottom under high pressures. We compared the learning behavior of two groups of college students before and after the use of visual aids: (1) geoscience majors and (2) non-geoscience major students. In general, the visual aid improved significantly the students' understanding of these geoscience processes, particularly for the non-geoscience students.